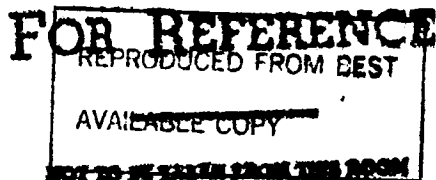


NASA Technical Memorandum 80131

NASA-TM-80131 19790025755

# Application of a Numerical Orthogonal Coordinate Generator to Axisymmetric Blunt Bodies

Randolph A. Graves, Jr.



OCTOBER 1979

LIBRARY COPY

OCT 30 1979

LANGLEY RESEARCH CENTER  
LIBRARY, NASA  
HAMPTON, VIRGINIA

NASA



# Application of a Numerical Orthogonal Coordinate Generator to Axisymmetric Blunt Bodies

Randolph A. Graves, Jr.  
*Langley Research Center*  
*Hampton, Virginia*



**Scientific and Technical  
Information Branch**



## SUMMARY

An application of a simple numerical technique which allows for the rapid construction of orthogonal coordinate systems about axisymmetric blunt bodies is presented. This technique can generate orthogonal meshes which have unequally spaced points in two directions. Relations are given for the numerical generation of the metric coefficients.

Body shapes ranging from simple analytical bodies to complex reverse curvature bodies are presented together with their orthogonal coordinate systems. The relatively good accuracy of the technique is shown in tabular data describing coordinate line slopes and metric coefficients. The "predictor-corrector" numerical method used to generate these results is both simple in concept and easy to program, so that the application of the technique should be broader than the results presented.

## INTRODUCTION

The introduction of high-speed computers with extensive memory capabilities has greatly enhanced the feasibility of solving the full Navier-Stokes equations for fluid flow over complex geometric shapes. One of the primary problems hindering the development of computational fluid dynamics for complex geometries has been the difficulty of generating the finite-difference mesh. A great deal of effort has been expended to develop coordinate transformations and/or mesh generators for varying degrees of geometric complexity. (See refs. 1 to 14.) These techniques range from the very simple, as in reference 1, to the mathematically elegant, as in reference 14. However, for flow over blunt entry bodies, it is imperative that the boundary conditions on the body be represented as accurately as possible by the finite-difference approximations to the Navier-Stokes equations, because the regions adjacent to solid surfaces generally dominate the character of the remaining flow field. The viscous shear stress forces on solid bodies depend directly on the large gradients (in the direction normal to the solid surface). Accurate skin-friction coefficients require that these large gradients be resolved accurately. Therefore, almost all numerical solutions to the Navier-Stokes equations to date have used body geometries conducive to use with natural or nearly orthogonal coordinate systems.

In the natural coordinate system, the body surface itself forms one boundary. That is, the body contour coincides with a constant coordinate line. Some simple examples of this approach are a cylindrical coordinate system to describe flow over a cylinder, a spherical coordinate system to describe flow over a sphere, and a parabolic coordinate system to describe the flow over a paraboloidal body. In each of these coordinate systems, the normal coordinates intersect the body orthogonally, thus simplifying the boundary conditions. There is little difficulty in compressing the mesh near the body because the computational mesh system is composed of lines parallel to the body which can be concentrated as close to the body as desired. There is, however, one rather severe restric-

tion on the natural coordinate system; that is, the body must have an analytic shape. Unfortunately, most realistic entry bodies bear little resemblance to the limited number of natural coordinate systems available.

Another option is similar to the natural coordinate system in that the body surface becomes one coordinate line in the system. This is called the body-oriented coordinate system. In this system the coordinates of a point are determined by the distance along a body surface measured from the axis of symmetry and the distance along a normal to the body. This type of system has been used to describe the flow over the forebody portions of blunt entry bodies. (See refs. 15 to 17 for examples.) The major problem with this system is that any discontinuity in slope on the body makes it impossible to describe the complete flow field. The body-oriented system, therefore, cannot handle the body shape with a concavity produced by heat-shield ablation in a severe heating environment.

Conformal mapping gives a well-developed and accurate alternate method of generating orthogonal coordinate systems for complicated geometric shapes. Reference 14 provides a recent look at some of the latest and most sophisticated techniques. Conformal mapping methods, however, are mathematically complicated and require multiple transformation steps leading to a loss of physical reality in the computational plane. Such complications make finite-difference mesh setups difficult.

Reference 12 presents a nearly orthogonal coordinate generator, somewhat similar to conformal mapping in concept, which has been used in two-dimensional and axisymmetric calculations; however, the technique is not easily applied and requires a great deal of user familiarity to execute successfully. One relatively easy analytic technique (ref. 10) has produced excellent results (ref. 18), but the technique is limited by the necessity of specifying the body shape by an analytical trigonometric series.

This paper presents a more general orthogonal coordinate system which can represent a wide range of body geometries. This technique is based on the rather simple but accurate numerical method developed in reference 19. The body can be represented by a series of discrete (but continuous) points rather than by an analytical approximation. In the transformed computational plane, the region of interest is rectangular, with the body surface being a coordinate line. This representation combines the advantages of the natural coordinate system and the generalized orthogonal coordinate system. In addition, generating the coordinates in the physical plane simplifies the finite-difference mesh setup.

#### SYMBOLS

$h_1, h_2, h_3$	metric coefficients for transformed coordinates
$h_{i,j}$	metric coefficient
i	tangential direction index

J	total number of mesh points in normal direction
j	normal direction index
K <sub>C</sub>	unequal spacing parameter
N	unequal spacing coordinate parameter
r <sub>l</sub>	local distance between body surface and outer boundary
r <sub>o</sub>	radius of outer circular boundary
r <sub>s</sub>	radius of body surface from its geometric center
u <sup>1</sup> , u <sup>2</sup> , u <sup>3</sup>	generalized transformed coordinates
x <sup>1</sup> , x <sup>2</sup> , x <sup>3</sup>	generalized coordinates
x, y, z	Cartesian coordinates
n, ξ, φ	transformed orthogonal coordinates
θ	internal body angle
θ <sub>o</sub>	outer circular boundary angle
θ <sub>l</sub>	local angle for r <sub>l</sub>
ρ	local radius from axis of symmetry

Subscripts:

o	outer boundary related quantities
s	body surface quantities

#### DESCRIPTION OF METHOD

For the mesh generation about an axisymmetric body, the origin of the x,y coordinate system is taken as the approximate center of the body. Once the body is described in terms of x,y points, then the surface distance  $\xi$  can be calculated in a generalized manner by defining  $\xi$  as 0 on the -y ordinate (see fig. 1) and  $\theta$  as increasing positively in the  $\xi$  direction. Then  $\xi$  is given by

$$\xi(\theta) = \int_0^\theta \left[ r_s^2 + \left( \frac{dr_s}{d\theta} \right)^2 \right]^{1/2} d\theta$$

where

$$r_s = (x_s^2 + y_s^2)^{1/2}$$

$$\theta = \sin^{-1} (x_s/r_s)$$

Once  $\xi$  is defined, the next step is to construct  $\eta$  level lines between the body and a suitable outer boundary. As pointed out in reference 11, a circular outer boundary simplifies the specification of the outer boundary conditions for fluid dynamic calculations. Most of the examples presented in this paper use a circular outer boundary. However, the outer boundary may be specified as any reasonable shape; and for those cases where only a partial field is to be described, one can use a discrete shock wave as the outer boundary. The circular boundary can be easily specified by a polar coordinate system where

$$x = r_o \cos \theta_o$$

$$y = r_o \sin \theta_o$$

In this system,  $r_o$  is the radius of the outer boundary and  $\theta_o$  is usually taken in equal increments around the outer boundary. On the outer boundary,  $\eta = 1$  while on the body  $\eta = 0$ . The level lines between the boundary and the body can be constructed along straight lines connecting corresponding points on the body and circular boundary. Note that the mesh points on the outer circular boundary are not the final mesh points, but initial values used only to set up the level lines. The spacing of the level lines can be unequal and the unequal spacing relation of reference 20 can be easily applied:

$$\eta_j = \frac{k_c^{N_j/\Delta N} - 1}{k_c^{1/\Delta N} - 1}$$

where  $N_j = (j - 1)\Delta N$  and  $N_J = 1$ , with  $\Delta N = 1/(J - 1)$  and  $k_c$  being the spacing parameter (generally  $1 < k_c < 2$ ). The larger the spacing parameter  $k_c$ , the more unequal the spacing. From the above relation, the level lines between all corresponding points on the body and circular boundary can be calculated. The relationships for the corresponding values of  $x, y$  can be obtained (see fig. 2 geometrical schematic) from

$$r_{l,i} = \left[ \frac{(x_{\eta=1} - x_{\eta=0})_i^2 + (y_{\eta=1} - y_{\eta=0})_i^2}{i} \right]^{1/2}$$

$$x_{i,j} = x_{i,\eta=0} + (\eta_j r_{l,i}) \cos (\theta_l)$$

$$y_{i,j} = y_{i,\eta=0} + (\eta_j r_{l,i}) \sin (\theta_l)$$

where

$$\theta_l = \sin^{-1} \left[ (y_{\eta=1} - y_{\eta=0}) / r_{l,i} \right]$$

Figure 3 shows the level lines constructed in this manner for an ellipse with  $K_C = 1.01$ , which gives nearly equal spacing.

Once the level lines have been determined, the normal lines are constructed so that an orthogonal system is defined. The approach to the construction of the normal lines is the one given in reference 18 which uses a simple "predictor-corrector" technique analogous to the trapezoidal integration technique of numerical integration. In this technique, the solution is first predicted from the level line at a known point by using the Euler method. Once the predicted point on the next level line is obtained, then the slope at that point is calculated and a new predicted point is obtained from this slope. The actual solution is then a combination of these two solutions; i.e., the final  $x$  and  $y$  values are an average of the predicted and corrected values. This procedure is illustrated in figure 4. The solution then proceeds point by point along a level line until all normals on that level have been constructed. Then the solution proceeds to the next level and the process is continued until the outer boundary is reached.

#### EXAMPLES OF COMPUTED COORDINATE SYSTEMS

Figures 5 to 7 show examples of the orthogonal coordinate systems constructed about three ellipses with increasing degrees of ellipticity. These solutions are for equal spacing both in the  $\xi$  and  $\eta$  directions. Notice the divergence of the coordinate lines in the regions of large curvature. This effect of curvature can be easily remedied through unequal spacing in the  $\xi$  direction as shown in figures 8 and 9. If unequal spacing is used in the  $\eta$  direction also, then a smoothly varying coordinate system with no region of rapid divergence of the coordinate lines results. (See fig. 10.)

A somewhat more realistic body is presented in figure 11. This body represents a typical planetary entry shape, and the coordinate system produced is quite good even though very little unequal spacing is used in the  $\xi$  direction. Figure 12 shows the same body, but with unequal ( $K_C = 1.08$ ) spacing in the  $\eta$  direction. Again, as in figure 10, the results are quite good.

To demonstrate the use of the coordinate generator on bodies with reverse curvature, the body shown in figure 13 was arbitrarily chosen. The reverse curvature poses no special problem; however, the normal coordinate lines tend

to converge. The effect is highly unequal spacing in the regions far from the body. The amount of reverse curvature here is relatively small; nevertheless, problems will probably occur on deeper cavity shapes. Figure 14 shows the same body with unequal ( $K_C = 1.08$ ) spacing in the  $\eta$  direction.

A natural compression of  $\eta$  lines occurs when the geometric center of the outer boundary is displaced in relation to the geometric center of the body, as shown in figures 15 and 16. For supersonic blunt body flows, the shifting of the outer boundary is highly desirable, since the shock wave is close to the body in the forward region and a compression of coordinate lines is necessary. The stretching of the level lines in the base is not detrimental, since the normal gradients in this region are not as strong as on the forebody.

All the above cases were run with 31  $\eta$  level lines and 100  $\xi$  normal lines giving 3000 points for the present analysis. Run times on the CYBER 175 computer averaged approximately 5 seconds, including compilation. On more complicated geometries, more points may be necessary. For cases where there is a symmetry plane in the field, only half as many points need to be used.

In addition to the whole body solutions given above, the coordinate generator can be used on partial bodies such as the forebody region on a blunt body. Figures 17 and 18 give solutions for partial bodies, with a representation of an ablated entry body with reverse curvature in the stagnation region shown in figure 18. This technique is sufficiently fast to make its use with an interactive graphics terminal both feasible and desirable.

#### COORDINATE METRICS

Since the intended use of the orthogonal coordinates generated using the present technique is for axisymmetric bodies, the following coordinate system (see fig. 19) will be used to generate the metrics, where the nomenclature follows that of reference 21:

$$u^1 = \eta \quad x^1 = \rho \cos \phi$$

$$u^2 = \xi \quad x^2 = \rho \sin \phi$$

$$u^3 = \phi \quad x^3 = z$$

where  $\rho = \rho(\xi, \eta)$ ;  $z = z(\xi, \eta)$  and the metric coefficients are given by

$$h_{i,j} = \frac{\partial x^1}{\partial u^i} \frac{\partial x^1}{\partial u^j} + \frac{\partial x^2}{\partial u^i} \frac{\partial x^2}{\partial u^j} + \frac{\partial x^3}{\partial u^i} \frac{\partial x^3}{\partial u^j}$$

For an orthogonal system, the metric coefficients

$$h_{1,2}, h_{2,1}, h_{1,3}, h_{3,1}, h_{2,3}, h_{3,2}$$

all have to be zero, leaving only the three familiar coefficients  $h_1, h_2, h_3$ , which are

$$h_1 = h_{1,1} \quad h_2 = h_{2,2} \quad h_3 = h_{3,3}$$

When the derivatives in the metric coefficient relation are taken, the following metric coefficient expressions are obtained:

$$h_{1,1} = \left( \frac{\partial \rho}{\partial \eta} \right)^2 + \left( \frac{\partial z}{\partial \eta} \right)^2$$

$$h_{1,2} = h_{2,1} = \frac{\partial \rho}{\partial \eta} \frac{\partial \rho}{\partial \xi} + \frac{\partial z}{\partial \eta} \frac{\partial z}{\partial \xi}$$

$$h_{1,3} = h_{3,1} = 0$$

$$h_{2,2} = \left( \frac{\partial \rho}{\partial \xi} \right)^2 + \left( \frac{\partial z}{\partial \xi} \right)^2$$

$$h_{2,3} = h_{3,2} = 0$$

$$h_{3,3} = \rho^2$$

With the choice of the present coordinate system, two of the three necessary orthogonality conditions are identically satisfied, leaving only the  $h_{1,2}$  coefficient to be evaluated numerically to determine the accuracy of the orthogonal coordinate generator. Table I presents results for the metric coefficients evaluated with second-order accurate derivative relations. Generally,  $h_{1,2}$  is relatively small compared with the other coefficients in spite of being a product of derivatives which amplifies errors. One has reasonable justification for ignoring the  $h_{1,2}$  coefficient and assuming orthogonality; thus only the three coefficients  $h_{1,1}$ ,  $h_{2,2}$ , and  $h_{3,3}$  are left. Orthogonality is also

indicated by comparison of the slopes of the level and normal lines at their intersection. Table II gives some typical results which indicate that the normal-line construction procedure does, in fact, give reasonably good results.

To test the effect of mesh size on the metric coefficients, a 1.5:1 ellipse was chosen with equal spacing along and normal to the body. The  $h_{1,1}$  metric coefficient on the body surface is given in table III for a range of mesh sizes. Because of symmetry, only the results for the first quadrant are presented. As expected, the results show that the metric coefficient does vary with mesh size; however, for the range of mesh points chosen, the variation is relatively small.

The only significant drawback to the numerical coordinate generator scheme is that the metric coefficients also must be numerically generated and thus stored at every point for future use. Since the metric values must be stored at each point, some computer storage limitations could result for very large or complex geometries.

#### CONCLUDING REMARKS

The results of the application of a simple "predictor-corrector" numerical technique which allowed rapid construction of orthogonal coordinate systems about axisymmetric blunt bodies have been shown. This technique generated orthogonal meshes which have unequally spaced points in two directions. The technique is general enough to allow for coordinate generation about bodies ranging from simple analytic shapes to more complex bodies with reverse curvature. The relatively good accuracy of the technique was demonstrated through the tabular data presented on coordinate line slopes and metric coefficients.

The predictor-corrector numerical technique used to generate results given in this paper is both simple in concept and easy to program, so that the use of the method should be broader than the limited application presented here. In fact, the method should lend itself to use with interactive graphic systems.

Langley Research Center  
National Aeronautics and Space Administration  
Hampton, VA 23665  
September 17, 1979

## REFERENCES

1. Amsden, A. A.; and Hirt, C. W.: A Simple Scheme for Generating General Curvilinear Grids. *J. Comput. Phys.*, vol. 11, no. 3, Mar. 1973, pp. 348-359.
2. Barfield, W. D.: Numerical Method for Generating Orthogonal Curvilinear Meshes. *J. Comput. Phys.*, vol. 5, no. 1, Feb. 1970, pp. 23-33.
3. Chu, Wen-Hwa: Development of a General Finite Difference Approximation for a General Domain. Part 1: Machine Transformation. *J. Comput. Phys.*, vol. 8, no. 3, Dec. 1971, pp. 392-408.
4. Starius, Göran: Constructing Orthogonal Curvilinear Meshes by Solving Initial Value Problems. *Numer. Math.*, vol. 28, Fasc. 1, 1977, pp. 25-48.
5. Gordon, William J.; and Hall, Charles A.: Construction of Curvilinear Co-Ordinate Systems and Applications to Mesh Generation. *Int. J. Numer. Methods Eng.*, vol. 7, no. 4, 1973, pp. 461-477.
6. Oberkampf, William L.: Domain Mappings for the Numerical Solution of Partial Differential Equations. *Int. J. Numer. Methods Eng.*, vol. 10, no. 1, 1976, pp. 211-223.
7. Marconi, F.; and Salas, M.: Computation of Three Dimensional Flows About Aircraft Configurations. *Comput. & Fluids*, vol. 1, no. 2, June 1973, pp. 185-195.
8. Caughey, D. A.: A Systematic Procedure for Generating Useful Conformal Mappings. *Int. J. Numer. Methods Eng.*, vol. 12, no. 11, 1978, pp. 1651-1657.
9. Starius, Göran: Composite Mesh Difference Methods for Elliptic Boundary Value Problems. *Numer. Math.*, vol. 28, Fasc. 2, 1977, pp. 243-258.
10. Gnoffo, Peter A.: A Generalized Orthogonal Coordinate System for Describing Families of Axisymmetric and Two-Dimensional Bodies. *NASA TM X-3468*, 1977.
11. Thompson, Joe F.; Thames, Frank C.; and Mastin, C. Wayne: Automatic Numerical Generation of Body-Fitted Curvilinear Coordinate System for Field Containing Any Number of Arbitrary Two-Dimensional Bodies. *J. Comput. Phys.*, vol. 15, no. 3, July 1974, pp. 299-319.
12. Hayes, John K.; Kahaner, David K.; and Kellner, Richard G.: An Improved Method for Numerical Conformal Mapping. *Math. Comput.*, vol. 26, no. 118, Apr. 1972, pp. 327-334.
13. Warschawski, S. E.: The Lichtenstein-Gershgorin Integral Equation in Conformal Mapping of Variable Domains. *J. Math. & Mech.*, vol. 19, no. 12, June 1970, pp. 1131-1153.

14. Ives, David C.: A Modern Look at Conformal Mapping Including Multiply Connected Regions. AIAA J., vol. 14, no. 8, Aug. 1976, pp. 1006-1011.
15. Graves, Randolph Anderson, Jr.: Solutions to the Navier-Stokes Equations for Supersonic Flow Over Blunt Bodies With Massive Wall Blowing. Ph. D. Diss., The George Washington Univ., 1977.
16. Moss, James N.: Reacting Viscous-Shock-Layer Solutions With Multicomponent Diffusion and Mass Injection. NASA TR R-411, 1974.
17. Kumar, Ajay; and Graves, R. A., Jr.: Numerical Solution of the Viscous Hypersonic Flow Past Blunted Cones at Angle of Attack. AIAA Paper No. 77-172, Jan. 1977.
18. Gnoffo, Peter A.: Forebody and Afterbody Solutions of the Navier-Stokes Equations for Supersonic Flow Over Blunt Bodies in a Generalized Orthogonal Coordinate System. NASA TP-1075, 1978.
19. McNally, William D.: FORTRAN Program for Generating a Two-Dimensional Orthogonal Mesh Between Two Arbitrary Boundaries. NASA TN D-6766, 1972.
20. Blottner, F. G.: Variable Grid Scheme Applied to Turbulent Boundary Layers. Comput. Methods Appl. Mech. & Eng., vol. 4, no. 2, Sept. 1974, pp. 179-194.
21. Wills, A. P.: Vector Analysis With an Introduction to Tensor Analysis. Dover Publ., Inc., c.1958.

TABLE I.- METRIC COEFFICIENTS

(a) Ellipse;  $\xi = 1.34$ 

$\eta$	$h_{1,1}$	$h_{1,2}$	$h_{2,2}$	$h_{3,3}$
0.	.29743E+02	-.52567E-02	.99942E+00	.79288E+00
.28748E+01	.31364E+02	-.37742E-02	.10479E+01	.10957E+01
.57784E+01	.32516E+02	-.45342E-02	.11085E+01	.14575E+01
.87110E+01	.33369E+02	-.31052E-02	.11810E+01	.18789E+01
.11673E+00	.34036E+02	-.19122E-02	.12637E+01	.23620E+01
.14664E+00	.34531E+02	-.77245E-03	.13567E+01	.29078E+01
.17686E+00	.34921E+02	-.12844E-02	.14601E+01	.35175E+01
.20738E+00	.35235E+02	-.45589E-03	.15733E+01	.41923E+01
.23820E+00	.35468E+02	.28407E-02	.16962E+01	.49334E+01
.26933E+00	.35648E+02	.23547E-02	.18298E+01	.57418E+01
.30077E+00	.35785E+02	.28811E-02	.19744E+01	.66185E+01
.33252E+00	.35887E+02	.30191E-02	.21301E+01	.75647E+01
.36460E+00	.35961E+02	.31352E-02	.22978E+01	.85815E+01
.39699E+00	.36013E+02	.32642E-02	.24778E+01	.96698E+01
.42971E+00	.36045E+02	.33919E-02	.26707E+01	.10831E+02
.46276E+00	.36062E+02	.35182E-02	.28771E+01	.12066E+02
.49613E+00	.36066E+02	.36504E-02	.30976E+01	.13375E+02
.52984E+00	.36058E+02	.37923E-02	.33329E+01	.14761E+02
.56389E+00	.36041E+02	.39460E-02	.35834E+01	.16224E+02
.59827E+00	.36015E+02	.41149E-02	.38500E+01	.17765E+02
.63300E+00	.35983E+02	.43034E-02	.41333E+01	.19385E+02
.66808E+00	.35944E+02	.45077E-02	.44339E+01	.21085E+02
.70351E+00	.35900E+02	.47217E-02	.47526E+01	.22867E+02
.73930E+00	.35851E+02	.55278E-02	.50899E+01	.24731E+02
.77544E+00	.35798E+02	.57440E-02	.54463E+01	.26679E+02
.81194E+00	.35741E+02	.59511E-02	.58229E+01	.28711E+02
.84881E+00	.35681E+02	.61450E-02	.62204E+01	.30829E+02
.88604E+00	.35618E+02	.63210E-02	.66397E+01	.33034E+02
.92365E+00	.35553E+02	.61864E-02	.70816E+01	.35326E+02
.96164E+00	.35485E+02	-.24348E-02	.75479E+01	.37708E+02
.10000E+01	.35415E+02	.43529E-02	.80379E+01	.40179E+02

TABLE I.- Continued

(b) Ellipse;  $\xi = 3.72$ 

$\eta$	$h_{1,1}$	$h_{1,2}$	$h_{2,2}$	$h_{3,3}$
0.	.13734E+02	-.23259E-02	.10015E+01	.11855E+00
.28748E+01	.14603E+02	-.98417E-02	.12334E+01	.18044E+00
.57784E+01	.15783E+02	-.15050E-01	.14551E+01	.25924E+00
.87110E+01	.16989E+02	-.17574E-01	.16732E+01	.35644E+00
.11673E+00	.18103E+02	-.17135E-01	.18931E+01	.47264E+00
.14664E+00	.19166E+02	-.18745E-01	.21178E+01	.60841E+00
.17686E+00	.20099E+02	-.18999E-01	.23488E+01	.76396E+00
.20738E+00	.20890E+02	-.21469E-01	.25891E+01	.93897E+00
.23820E+00	.21579E+02	-.22150E-01	.28395E+01	.11332E+01
.26933E+00	.22157E+02	-.22886E-01	.31017E+01	.13461E+01
.30077E+00	.22661E+02	-.26141E-01	.33767E+01	.15771E+01
.33252E+00	.23061E+02	-.25614E-01	.36654E+01	.18256E+01
.36460E+00	.23365E+02	-.25999E-01	.39688E+01	.20907E+01
.39699E+00	.23626E+02	-.27222E-01	.42876E+01	.23720E+01
.42971E+00	.23832E+02	-.30534E-01	.46227E+01	.26686E+01
.46276E+00	.23993E+02	-.31279E-01	.49736E+01	.29800E+01
.49613E+00	.24116E+02	-.32475E-01	.53413E+01	.33055E+01
.52984E+00	.24206E+02	-.33566E-01	.57260E+01	.36445E+01
.56389E+00	.24268E+02	-.34621E-01	.61281E+01	.39960E+01
.59827E+00	.24307E+02	-.35640E-01	.65479E+01	.43598E+01
.63300E+00	.24326E+02	-.36626E-01	.69857E+01	.47351E+01
.66808E+00	.24328E+02	-.37578E-01	.74416E+01	.51214E+01
.70351E+00	.24316E+02	-.38494E-01	.79159E+01	.55180E+01
.73930E+00	.24291E+02	-.39375E-01	.84087E+01	.59245E+01
.77544E+00	.24256E+02	-.40218E-01	.89204E+01	.63402E+01
.81194E+00	.24213E+02	-.41022E-01	.94511E+01	.67647E+01
.84881E+00	.24162E+02	-.41786E-01	.10001E+02	.71974E+01
.88604E+00	.24104E+02	-.42508E-01	.10570E+02	.76378E+01
.92365E+00	.24042E+02	-.43188E-01	.11158E+02	.80855E+01
.96164E+00	.23975E+02	-.43823E-01	.11767E+02	.85399E+01
.10000E+01	.23904E+02	-.44419E-01	.12395E+02	.90007E+01

TABLE I.- Continued

(c) Sphere;  $\xi = 0.823$ 

$\eta$	$h_{1,1}$	$h_{1,2}$	$h_{2,2}$	$h_{3,3}$
0.	.80002E+01	.26519E-02	.99971E+00	.46264E+00
.28748E+01	.80003E+01	.29355E-02	.11717E+01	.54085E+00
.57784E+01	.80004E+01	.32236E-02	.13592E+01	.62604E+00
.87110E+01	.80004E+01	.35155E-02	.15626E+01	.71839E+00
.11673E+00	.80005E+01	.38108E-02	.17824E+01	.81810E+00
.14664E+00	.80005E+01	.41094E-02	.20189E+01	.92538E+00
.17686E+00	.80005E+01	.44111E-02	.22727E+01	.10404E+01
.20738E+00	.80005E+01	.47156E-02	.25443E+01	.11634E+01
.23820E+00	.80006E+01	.50231E-02	.28340E+01	.12947E+01
.26933E+00	.80006E+01	.53332E-02	.31425E+01	.14343E+01
.30077E+00	.80006E+01	.56461E-02	.34701E+01	.15826E+01
.33252E+00	.80006E+01	.59616E-02	.38174E+01	.17398E+01
.36460E+00	.80006E+01	.62797E-02	.41850E+01	.19061E+01
.39699E+00	.80006E+01	.66005E-02	.45733E+01	.20817E+01
.42971E+00	.80006E+01	.69238E-02	.49830E+01	.22669E+01
.46276E+00	.80006E+01	.72497E-02	.54145E+01	.24620E+01
.49613E+00	.80006E+01	.75781E-02	.58685E+01	.26672E+01
.52984E+00	.80006E+01	.79092E-02	.63454E+01	.28828E+01
.56389E+00	.80006E+01	.82428E-02	.68461E+01	.31091E+01
.59827E+00	.80006E+01	.85790E-02	.73709E+01	.33462E+01
.63300E+00	.80006E+01	.89178E-02	.79207E+01	.35946E+01
.66808E+00	.80007E+01	.92592E-02	.84959E+01	.38544E+01
.70351E+00	.80007E+01	.96032E-02	.90973E+01	.41261E+01
.73930E+00	.80007E+01	.99499E-02	.97255E+01	.44099E+01
.77544E+00	.80007E+01	.10299E-01	.10381E+02	.47060E+01
.81194E+00	.80007E+01	.10651E-01	.11065E+02	.50149E+01
.84881E+00	.80007E+01	.11006E-01	.11778E+02	.53368E+01
.88604E+00	.80007E+01	.11363E-01	.12521E+02	.56721E+01
.92365E+00	.80007E+01	.11723E-01	.13294E+02	.60211E+01
.96164E+00	.80007E+01	.12086E-01	.14098E+02	.63841E+01
.10000E+01	.80007E+01	.12452E-01	.14934E+02	.67616E+01

TABLE I.- Continued

(d) Sphere;  $\xi = 2.07$ 

$\eta$	$h_{1,1}$	$h_{1,2}$	$h_{2,2}$	$h_{3,3}$
0.	.80015E+01	-.19233E-02	.99955E+00	.81405E+00
.28748E+01	.80015E+01	-.26334E-02	.11847E+01	.95217E+00
.57784E+01	.80015E+01	-.33281E-02	.13872E+01	.11026E+01
.87110E+01	.80015E+01	-.40103E-02	.16075E+01	.12658E+01
.11673E+00	.80015E+01	-.46825E-02	.18461E+01	.14420E+01
.14664E+00	.80015E+01	-.53466E-02	.21034E+01	.16310E+01
.17686E+00	.80015E+01	-.60041E-02	.23799E+01	.18350E+01
.20738E+00	.80015E+01	-.66560E-02	.26760E+01	.20524E+01
.23820E+00	.80015E+01	-.73031E-02	.29922E+01	.22845E+01
.26933E+00	.80015E+01	-.79460E-02	.33291E+01	.25314E+01
.30077E+00	.80015E+01	-.85853E-02	.36870E+01	.27936E+01
.33252E+00	.80015E+01	-.92214E-02	.40666E+01	.30716E+01
.36460E+00	.80015E+01	-.98545E-02	.44683E+01	.33657E+01
.39699E+00	.80015E+01	-.10485E-01	.48928E+01	.36764E+01
.42971E+00	.80014E+01	-.11113E-01	.53405E+01	.40041E+01
.46276E+00	.80014E+01	-.11739E-01	.58120E+01	.43493E+01
.49613E+00	.80014E+01	-.12363E-01	.63080E+01	.47124E+01
.52984E+00	.80014E+01	-.12985E-01	.68289E+01	.50938E+01
.56389E+00	.80014E+01	-.13605E-01	.73754E+01	.54941E+01
.59827E+00	.80014E+01	-.14223E-01	.79482E+01	.59138E+01
.63300E+00	.80014E+01	-.14839E-01	.85478E+01	.63534E+01
.66808E+00	.80014E+01	-.15454E-01	.91749E+01	.68133E+01
.70351E+00	.80014E+01	-.16067E-01	.98301E+01	.72941E+01
.73930E+00	.80014E+01	-.16679E-01	.10514E+02	.77963E+01
.77544E+00	.80014E+01	-.17289E-01	.11228E+02	.83205E+01
.81194E+00	.80014E+01	-.17898E-01	.11972E+02	.88672E+01
.84881E+00	.80014E+01	-.18505E-01	.12746E+02	.94371E+01
.88604E+00	.80014E+01	-.19111E-01	.13553E+02	.10031E+02
.92365E+00	.80014E+01	-.19715E-01	.14392E+02	.10648E+02
.96164E+00	.80014E+01	-.20317E-01	.15264E+02	.11291E+02
.10000E+01	.80014E+01	-.20918E-01	.16170E+02	.11959E+02

TABLE I.- Continued

(e) Blunt body;  $\xi = 0.791$ 

$\eta$	$h_{1,1}$	$h_{1,2}$	$h_{2,2}$	$h_{3,3}$
0.	.98722E+01	.26070E-03	.88007E+00	.44081E+01
.28748E+01	.98870E+01	.23573E-03	.91666E+00	.47425E+01
.57784E+01	.98962E+01	.18683E-03	.95728E+00	.50949E+01
.87110E+01	.99009E+01	.15985E-03	.10018E+01	.54658E+01
.11673E+00	.99021E+01	.14185E-03	.10501E+01	.58557E+01
.14664E+00	.99006E+01	.13135E-03	.11022E+01	.62649E+01
.17686E+00	.98967E+01	.12734E-03	.11581E+01	.66941E+01
.20738E+00	.98910E+01	.12903E-03	.12177E+01	.71437E+01
.23820E+00	.98837E+01	.13578E-03	.12812E+01	.76143E+01
.26933E+00	.98751E+01	.14704E-03	.13485E+01	.81065E+01
.30077E+00	.98655E+01	.16228E-03	.14198E+01	.86207E+01
.33252E+00	.98549E+01	.18094E-03	.14951E+01	.91576E+01
.36460E+00	.98436E+01	.20245E-03	.15745E+01	.97179E+01
.39699E+00	.98315E+01	.22620E-03	.16580E+01	.10302E+02
.42971E+00	.98189E+01	.25486E-03	.17458E+01	.10911E+02
.46276E+00	.98058E+01	.28456E-03	.18379E+01	.11545E+02
.49613E+00	.97923E+01	.48442E-03	.19345E+01	.12204E+02
.52984E+00	.97784E+01	.52308E-03	.20359E+01	.12891E+02
.56384E+00	.97641E+01	.55614E-03	.21420E+01	.13604E+02
.59827E+00	.97496E+01	.58160E-03	.22528E+01	.14346E+02
.63300E+00	.97348E+01	.53797E-03	.23687E+01	.15116E+02
.66808E+00	.97198E+01	-.98472E-03	.24895E+01	.15915E+02
.70351E+00	.97046E+01	-.61374E-03	.26157E+01	.16745E+02
.73930E+00	.96892E+01	-.72091E-03	.27471E+01	.17605E+02
.77544E+00	.96755E+01	-.79506E-03	.28840E+01	.18497E+02
.81194E+00	.96451E+01	-.57918E-03	.30263E+01	.19422E+02
.84881E+00	.96283E+01	-.36024E-03	.31743E+01	.20379E+02
.88604E+00	.96271E+01	-.38499E-03	.33274E+01	.21370E+02
.92365E+00	.96097E+01	-.37987E-03	.34863E+01	.22397E+02
.96164E+00	.95941E+01	-.35825E-03	.36511E+01	.23460E+02
.10000E+01	.95785E+01	-.32303E-03	.38219E+01	.24559E+02

TABLE I.- Concluded

(f) Blunt body;  $\xi = 4.28$ 

$\eta$	$h_{1,1}$	$h_{1,2}$	$h_{2,2}$	$h_{3,3}$
0.	.11203E+02	.26413E-02	.10913E+01	.14884E+01
.28748E+01	.11199E+02	.28560E-02	.12241E+01	.16167E+01
.57784E+01	.11193E+02	.33395E-02	.13649E+01	.17527E+01
.87110E+01	.11195E+02	.37638E-02	.15138E+01	.18968E+01
.11673E+00	.11194E+02	.67931E-02	.16711E+01	.20491E+01
.14664E+00	.11188E+02	.32156E-02	.18362E+01	.22098E+01
.17686E+00	.11187E+02	.49259E-02	.20100E+01	.23793E+01
.20738E+00	.11186E+02	.47386E-02	.21917E+01	.25579E+01
.23820E+00	.11186E+02	.46724E-02	.23821E+01	.27458E+01
.26933E+00	.11185E+02	.46309E-02	.25812E+01	.29433E+01
.30077E+00	.11185E+02	.46268E-02	.27892E+01	.31507E+01
.33252E+00	.11185E+02	.46710E-02	.30064E+01	.33683E+01
.36460E+00	.11185E+02	.47717E-02	.32330E+01	.35965E+01
.39699E+00	.11185E+02	.49350E-02	.34692E+01	.38355E+01
.42971E+00	.11186E+02	.52630E-02	.37153E+01	.40856E+01
.46276E+00	.11181E+02	.76549E-02	.39721E+01	.43473E+01
.49613E+00	.11221E+02	.78449E-02	.42393E+01	.46206E+01
.52984E+00	.11221E+02	.80243E-02	.45184E+01	.49068E+01
.56389E+00	.11180E+02	.85494E-02	.48100E+01	.52048E+01
.59827E+00	.11184E+02	.62666E-02	.51137E+01	.55156E+01
.63300E+00	.11183E+02	.68510E-02	.54287E+01	.58397E+01
.66808E+00	.11182E+02	.68398E-02	.57556E+01	.61774E+01
.70351E+00	.11181E+02	.69349E-02	.60947E+01	.65290E+01
.73930E+00	.11180E+02	.70617E-02	.64463E+01	.68950E+01
.77544E+00	.11180E+02	.77385E-02	.68107E+01	.72758E+01
.81194E+00	.11179E+02	.78999E-02	.71878E+01	.76717E+01
.84881E+00	.11179E+02	.80783E-02	.75784E+01	.80833E+01
.88604E+00	.11178E+02	.82904E-02	.79828E+01	.85109E+01
.92365E+00	.11178E+02	.85405E-02	.84016E+01	.89550E+01
.96164E+00	.11178E+02	.88303E-02	.88351E+01	.94161E+01
.10000E+01	.11177E+02	.91693E-02	.92839E+01	.98945E+01

TABLE II.- COORDINATE LINE SLOPES

## (a) Ellipse

$\eta$	$\xi = 1.34$		$\xi = 3.72$	
	$(dy/dx)_\eta$	$-1/(dy/dx)_\xi$	$(dy/dx)_\eta$	$-1/(dy/dx)_\xi$
.28748E+01	.20326E+00	.19924E+00	.91493E+00	.89472E+00
.57784E-01	.23216E+00	.22923E+00	.91737E+00	.90105E+00
.87110E-01	.25683E+00	.25473E+00	.93828E+00	.92348E+00
.11673E+00	.27847E+00	.27684E+00	.96974E+00	.95540E+00
.14664E+00	.29768E+00	.29632E+00	.10069E+01	.99317E+00
.17686E+00	.31519E+00	.31387E+00	.10481E+01	.10346E+01
.20738E+00	.33129E+00	.33012E+00	.10911E+01	.10782E+01
.23820E+00	.34586E+00	.34510E+00	.11360E+01	.11231E+01
.26933E+00	.35988E+00	.35911E+00	.11819E+01	.11690E+01
.30077E+00	.37314E+00	.37244E+00	.12284E+01	.12159E+01
.33252E+00	.38577E+00	.38513E+00	.12763E+01	.12631E+01
.36460E+00	.39788E+00	.39728E+00	.13236E+01	.13100E+01
.39699E+00	.40955E+00	.40899E+00	.13711E+01	.13570E+01
.42971E+00	.42085E+00	.42032E+00	.14182E+01	.14041E+01
.46276E+00	.43184E+00	.43133E+00	.14662E+01	.14514E+01
.49613E+00	.44257E+00	.44208E+00	.15145E+01	.14991E+01
.52984E+00	.45308E+00	.45259E+00	.15632E+01	.15470E+01
.56389E+00	.46340E+00	.46292E+00	.16123E+01	.15953E+01
.59827E+00	.47355E+00	.47308E+00	.16620E+01	.16441E+01
.63300E+00	.48358E+00	.48311E+00	.17121E+01	.16933E+01
.66808E+00	.49348E+00	.49302E+00	.17629E+01	.17430E+01
.70351E+00	.50329E+00	.50283E+00	.18143E+01	.17933E+01
.73930E+00	.51302E+00	.51255E+00	.18664E+01	.18443E+01
.77544E+00	.52269E+00	.52221E+00	.19193E+01	.18960E+01
.81194E+00	.53230E+00	.53181E+00	.19730E+01	.19484E+01
.84881E+00	.54186E+00	.54136E+00	.20276E+01	.20017E+01
.88604E+00	.55139E+00	.55087E+00	.20832E+01	.20558E+01
.92365E+00	.56089E+00	.56035E+00	.21398E+01	.21108E+01
.96164E+00	.57095E+00	.56995E+00	.21974E+01	.21668E+01

TABLE II.- Continued

## (b) Sphere

$\eta$	$\xi = 0.823$		$\xi = 2.07$	
	$(dy/dx)_\eta$	$-1/(dy/dx)_\xi$	$(dy/dx)_\eta$	$-1/(dy/dx)_\xi$
.28748E+01	.10821E+01	.10799E+01	.18585E+01	.18422E+01
.57784E+01	.10823E+01	.10801E+01	.18583E+01	.18419E+01
.87110E+01	.10825E+01	.10802E+01	.18582E+01	.18416E+01
.11673E+00	.10826E+01	.10804E+01	.18580E+01	.18413E+01
.14664E+00	.10828E+01	.10805E+01	.18578E+01	.18410E+01
.17686E+00	.10830E+01	.10807E+01	.18577E+01	.18407E+01
.20738E+00	.10831E+01	.10808E+01	.18575E+01	.18405E+01
.23820E+00	.10832E+01	.10809E+01	.18574E+01	.18402E+01
.26933E+00	.10834E+01	.10811E+01	.18573E+01	.18400E+01
.30077E+00	.10835E+01	.10812E+01	.18571E+01	.18398E+01
.33252E+00	.10836E+01	.10813E+01	.18570E+01	.18396E+01
.36460E+00	.10837E+01	.10814E+01	.18568E+01	.18394E+01
.39699E+00	.10838E+01	.10815E+01	.18567E+01	.18392E+01
.42971E+00	.10839E+01	.10816E+01	.18566E+01	.18390E+01
.46276E+00	.10840E+01	.10817E+01	.18565E+01	.18388E+01
.49613E+00	.10841E+01	.10818E+01	.18563E+01	.18386E+01
.52984E+00	.10842E+01	.10819E+01	.18562E+01	.18385E+01
.56389E+00	.10843E+01	.10820E+01	.18561E+01	.18383E+01
.59827E+00	.10844E+01	.10821E+01	.18560E+01	.18381E+01
.63300E+00	.10845E+01	.10822E+01	.18558E+01	.18380E+01
.66808E+00	.10846E+01	.10823E+01	.18557E+01	.18378E+01
.70351E+00	.10847E+01	.10823E+01	.18556E+01	.18377E+01
.73930E+00	.10848E+01	.10824E+01	.18555E+01	.18375E+01
.77544E+00	.10849E+01	.10825E+01	.18554E+01	.18374E+01
.81194E+00	.10849E+01	.10826E+01	.18553E+01	.18372E+01
.84881E+00	.10850E+01	.10827E+01	.18552E+01	.18371E+01
.88604E+00	.10851E+01	.10827E+01	.18551E+01	.18370E+01
.92365E+00	.10852E+01	.10828E+01	.18550E+01	.18368E+01
.96164E+00	.10852E+01	.10829E+01	.18548E+01	.18367E+01

TABLE II.- Concluded

## (c) Blunt body

$\eta$	$\xi = 0.791$		$\xi = 4.28$	
	$(dy/dx)_\eta$	$-1/(dy/dx)_\xi$	$(dy/dx)_\eta$	$-1/(dy/dx)_\xi$
.28748E+01	.57241E+00	.57270E+00	.15944E+01	.15695E+01
.57784E+01	.55953E+00	.55977E+00	.15759E+01	.15521E+01
.87110E+01	.54757E+00	.54776E+00	.15590E+01	.15365E+01
.11673E+00	.53637E+00	.53652E+00	.15459E+01	.15234E+01
.14664E+00	.52579E+00	.52591E+00	.15290E+01	.15107E+01
.17686E+00	.51574E+00	.51583E+00	.15158E+01	.14978E+01
.20738E+00	.50615E+00	.50622E+00	.15036E+01	.14861E+01
.23820E+00	.49696E+00	.49701E+00	.14922E+01	.14752E+01
.26933E+00	.48812E+00	.48814E+00	.14815E+01	.14649E+01
.30077E+00	.47958E+00	.47959E+00	.14715E+01	.14552E+01
.33252E+00	.47131E+00	.47131E+00	.14621E+01	.14460E+01
.36460E+00	.46329E+00	.46328E+00	.14532E+01	.14373E+01
.39699E+00	.45550E+00	.45547E+00	.14448E+01	.14291E+01
.42971E+00	.44791E+00	.44787E+00	.14368E+01	.14213E+01
.46276E+00	.44050E+00	.44045E+00	.14300E+01	.14141E+01
.49613E+00	.43327E+00	.43321E+00	.14228E+01	.14074E+01
.52984E+00	.42620E+00	.42613E+00	.14165E+01	.14007E+01
.56389E+00	.41928E+00	.41921E+00	.14098E+01	.13941E+01
.59827E+00	.41251E+00	.41242E+00	.14023E+01	.13876E+01
.63300E+00	.40587E+00	.40576E+00	.13960E+01	.13814E+01
.66808E+00	.39970E+00	.39933E+00	.13900E+01	.13755E+01
.70351E+00	.39332E+00	.39301E+00	.13841E+01	.13698E+01
.73930E+00	.38704E+00	.38673E+00	.13784E+01	.13643E+01
.77544E+00	.38088E+00	.38055E+00	.13729E+01	.13590E+01
.81194E+00	.37481E+00	.37451E+00	.13676E+01	.13539E+01
.84881E+00	.36884E+00	.36858E+00	.13624E+01	.13489E+01
.88604E+00	.36296E+00	.36269E+00	.13574E+01	.13440E+01
.92365E+00	.35717E+00	.35689E+00	.13525E+01	.13392E+01
.96164E+00	.35147E+00	.35118E+00	.13478E+01	.13346E+01

TABLE III.- METRIC COEFFICIENT AS FUNCTION OF MESH SIZE  
FOR 1.5:1 ELLIPSE

$\xi$	h <sub>1,1</sub> for coordinate mesh size of -					
	101 × 41	101 × 31	101 × 21	51 × 41	51 × 31	51 × 21
0	13.000	13.000	13.000	13.000	13.000	13.000
.159	12.996	12.996	12.996	12.996	12.996	12.996
.317	12.567	12.568	12.570	12.581	12.581	12.583
.456	12.349	12.349	12.350	12.190	12.190	12.192
.635	11.842	11.843	11.846	11.750	11.750	11.753
.793	11.344	11.345	11.349	11.247	11.248	11.251
.872	10.796	10.797	10.831	10.668	10.669	10.673
.912	10.302	10.303	10.324	10.137	10.138	10.142
1.031	9.857	9.858	9.862	9.686	9.686	9.690
1.189	9.555	9.556	9.597	9.366	9.366	9.369
1.348	9.414	9.414	9.432	9.239	9.239	9.241
1.507	9.453	9.453	9.454	9.315	9.316	9.317
1.666	9.583	9.583	9.584	9.524	9.524	9.525

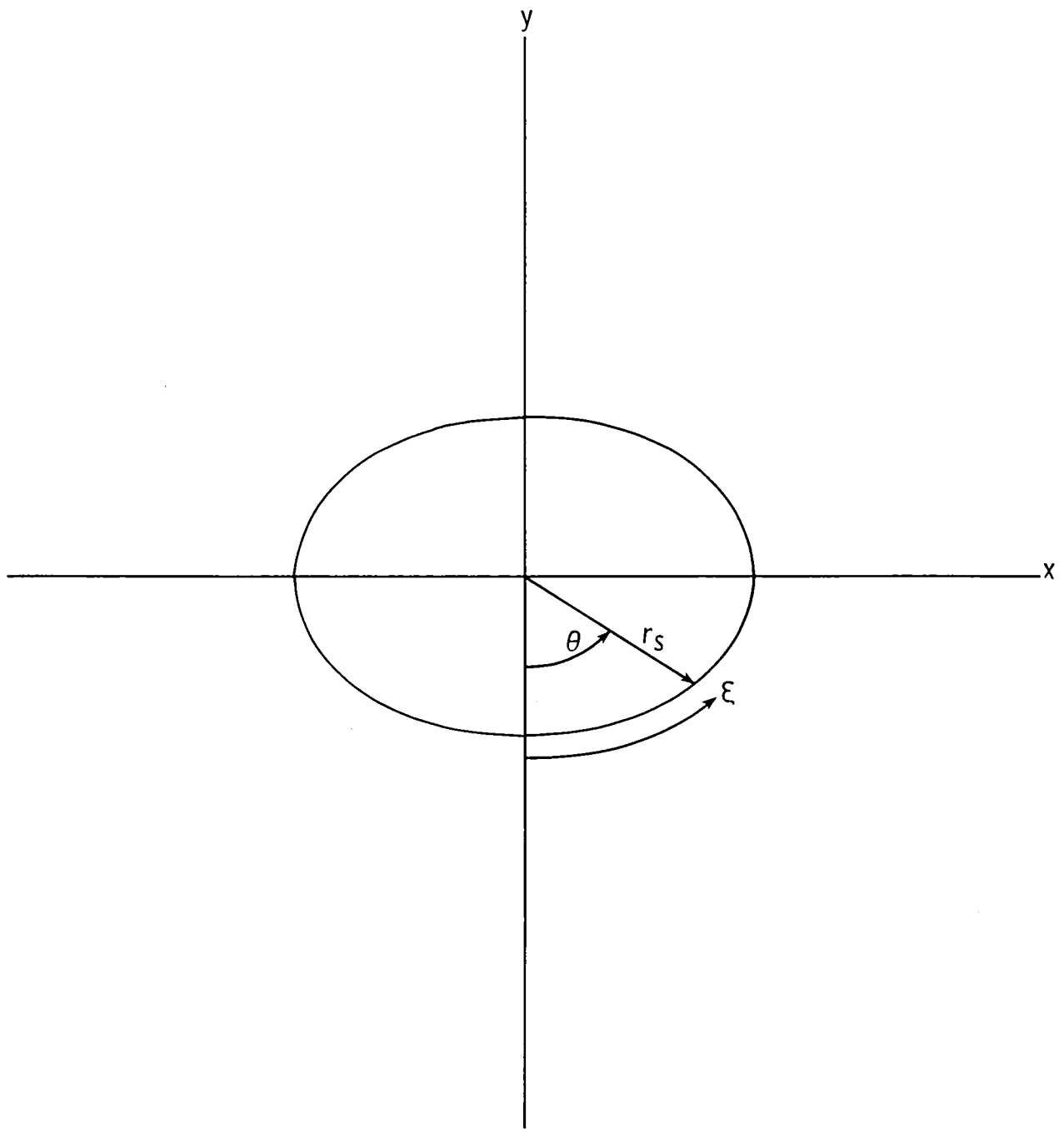


Figure 1.- Body surface geometry.

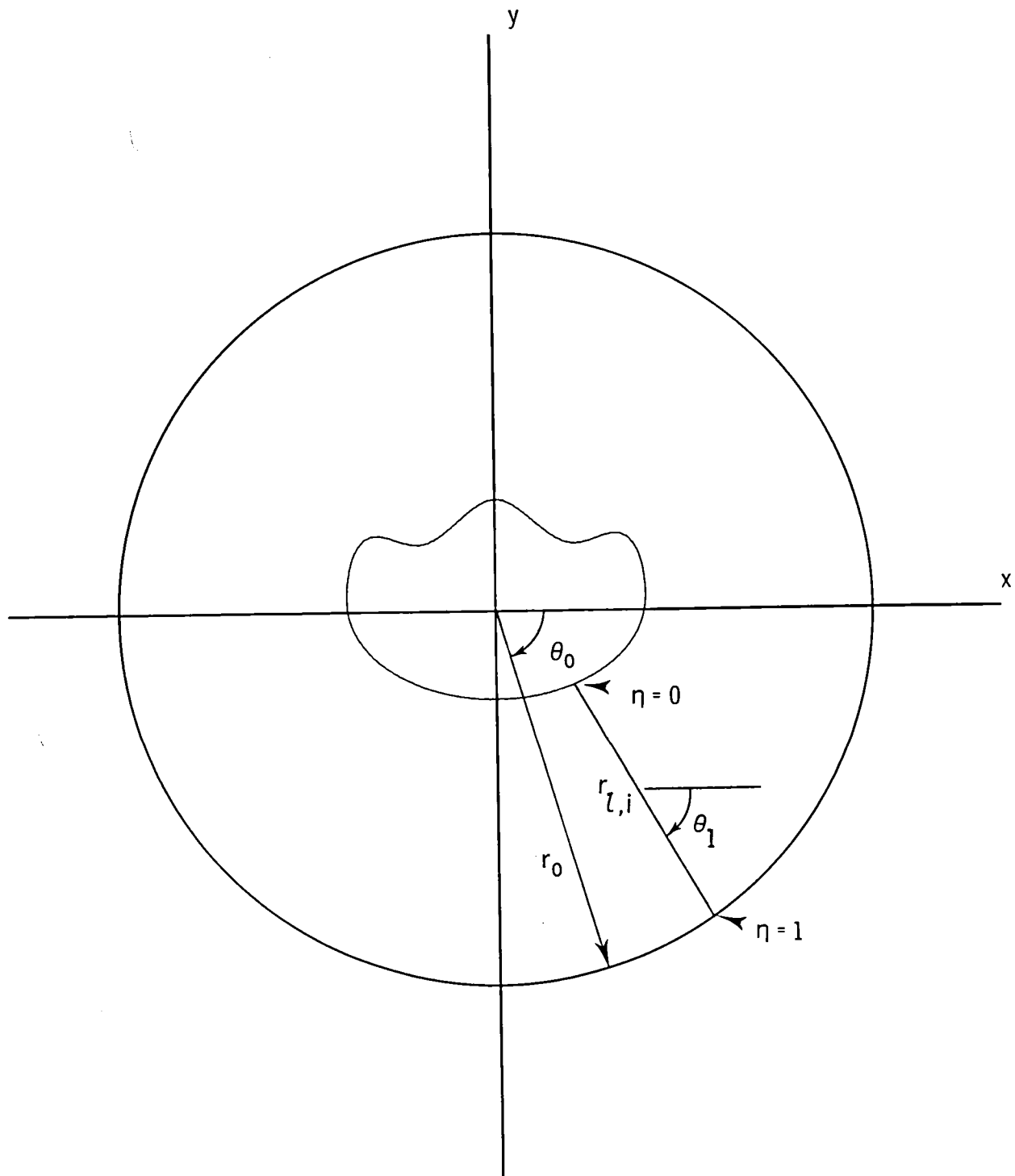
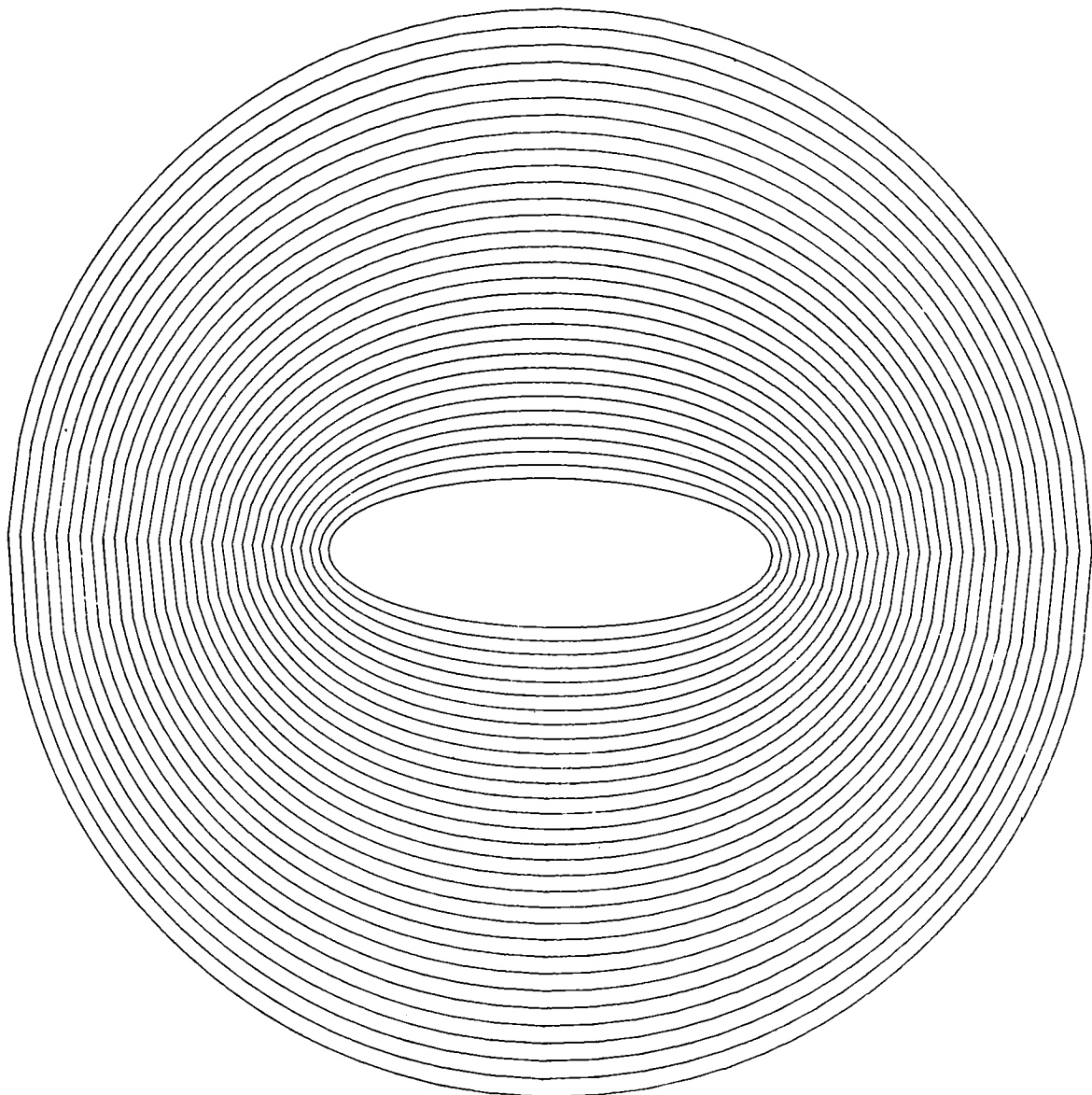


Figure 2.- Geometry of body and outer boundary.



**Figure 3.- Level lines about ellipsoid.**

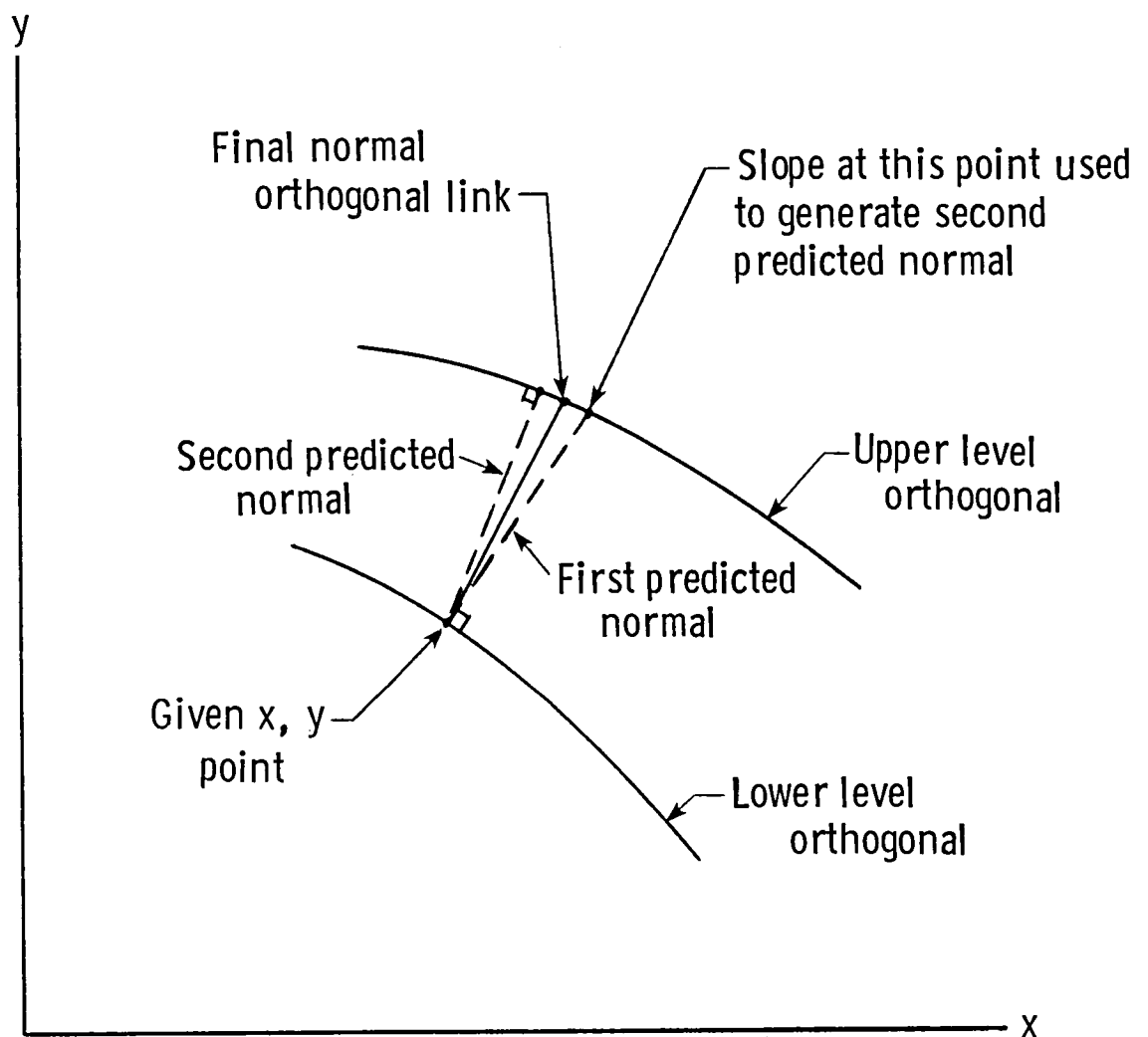


Figure 4.- Calculation procedure for normal orthogonal link.

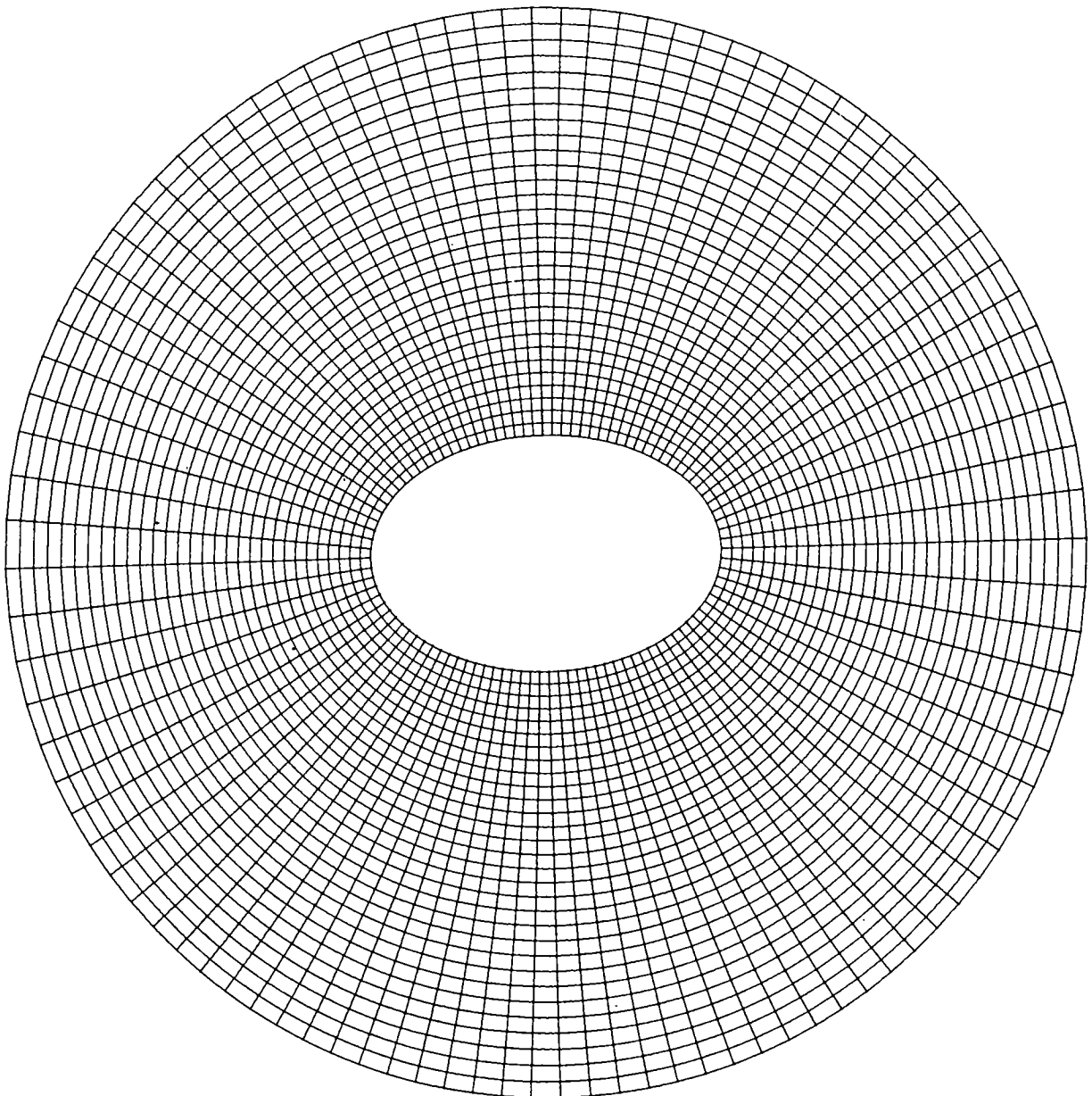


Figure 5.- Orthogonal coordinate system about 1.5:1 ellipsoid with equal  $\xi$  spacing.

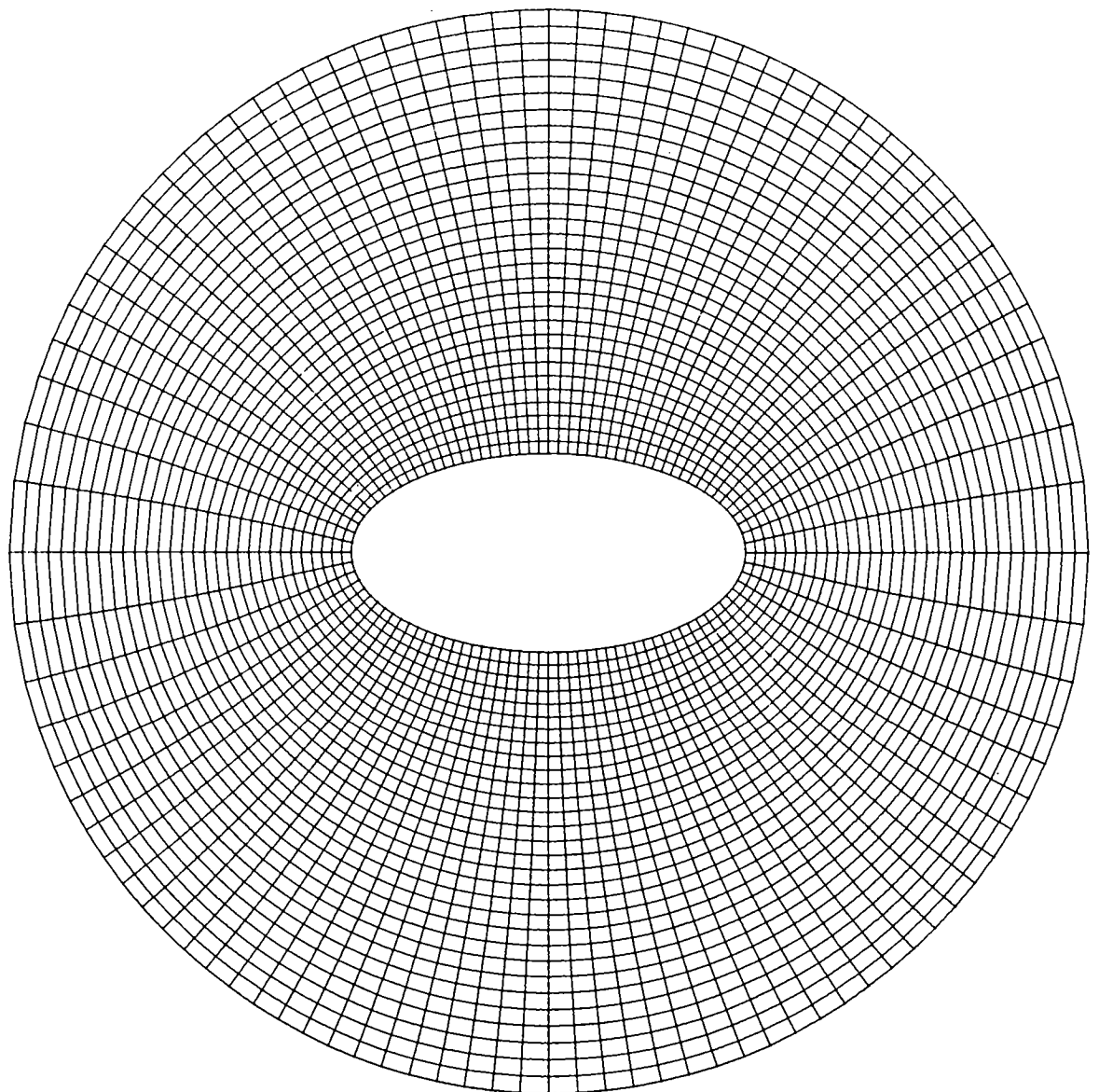


Figure 6.- Orthogonal coordinate system about 2:1 ellipsoid with equal  $\xi$  spacing.

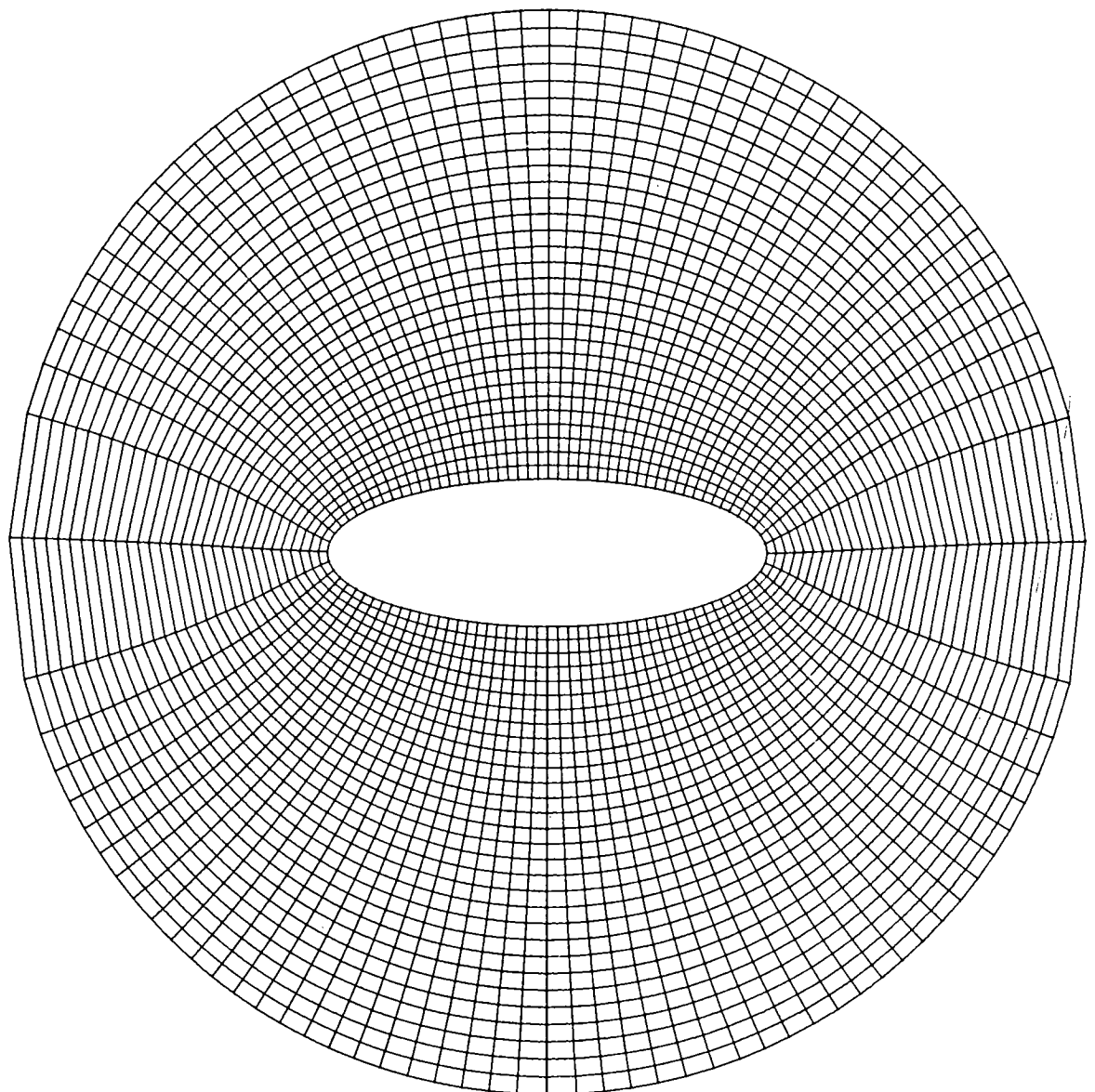
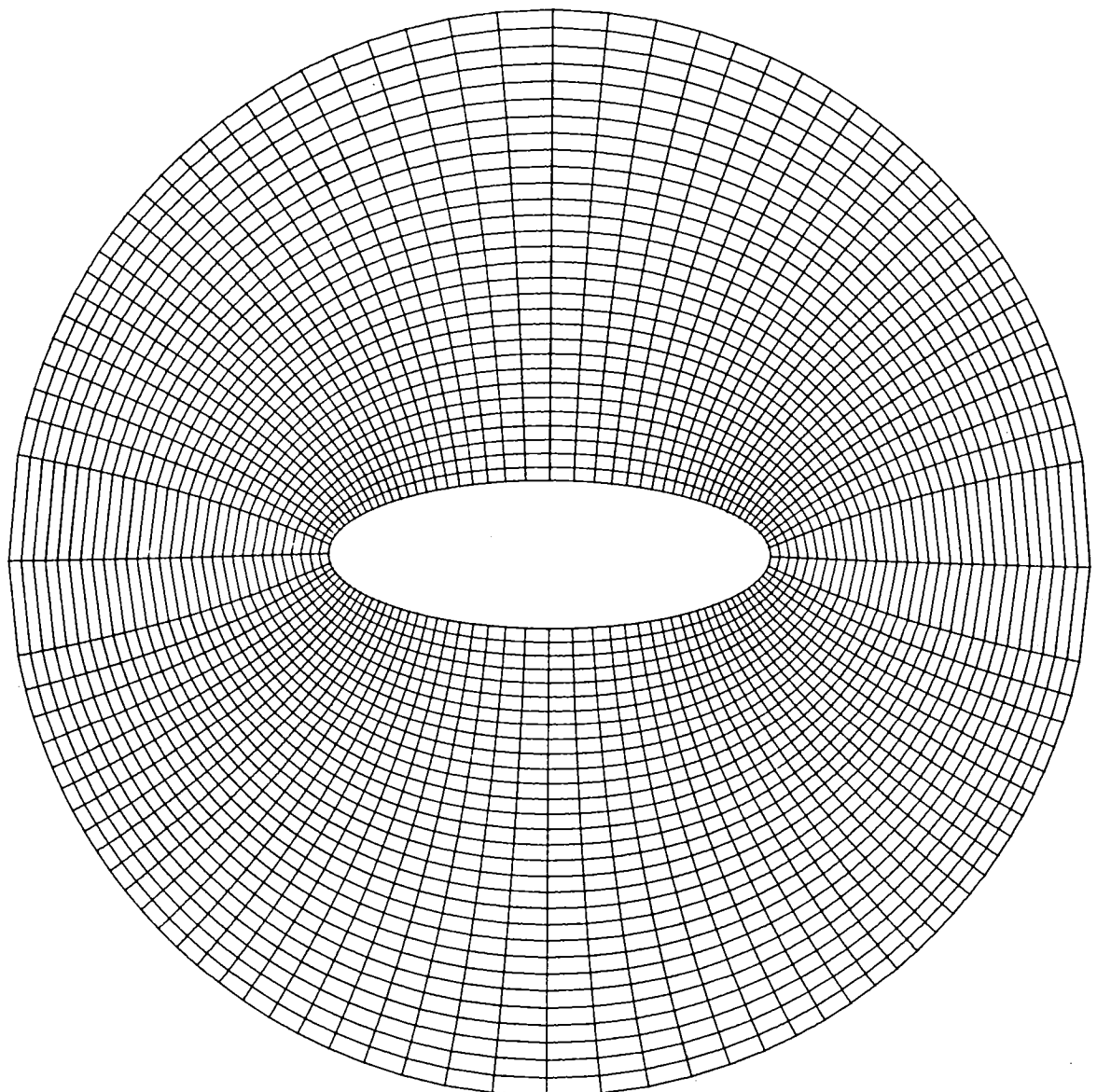


Figure 7.- Orthogonal coordinate system about 3:1 ellipsoid with equal  $\xi$  spacing.



**Figure 8.-** Orthogonal coordinate system about 3:1 ellipsoid with slightly unequal  $\xi$  spacing.

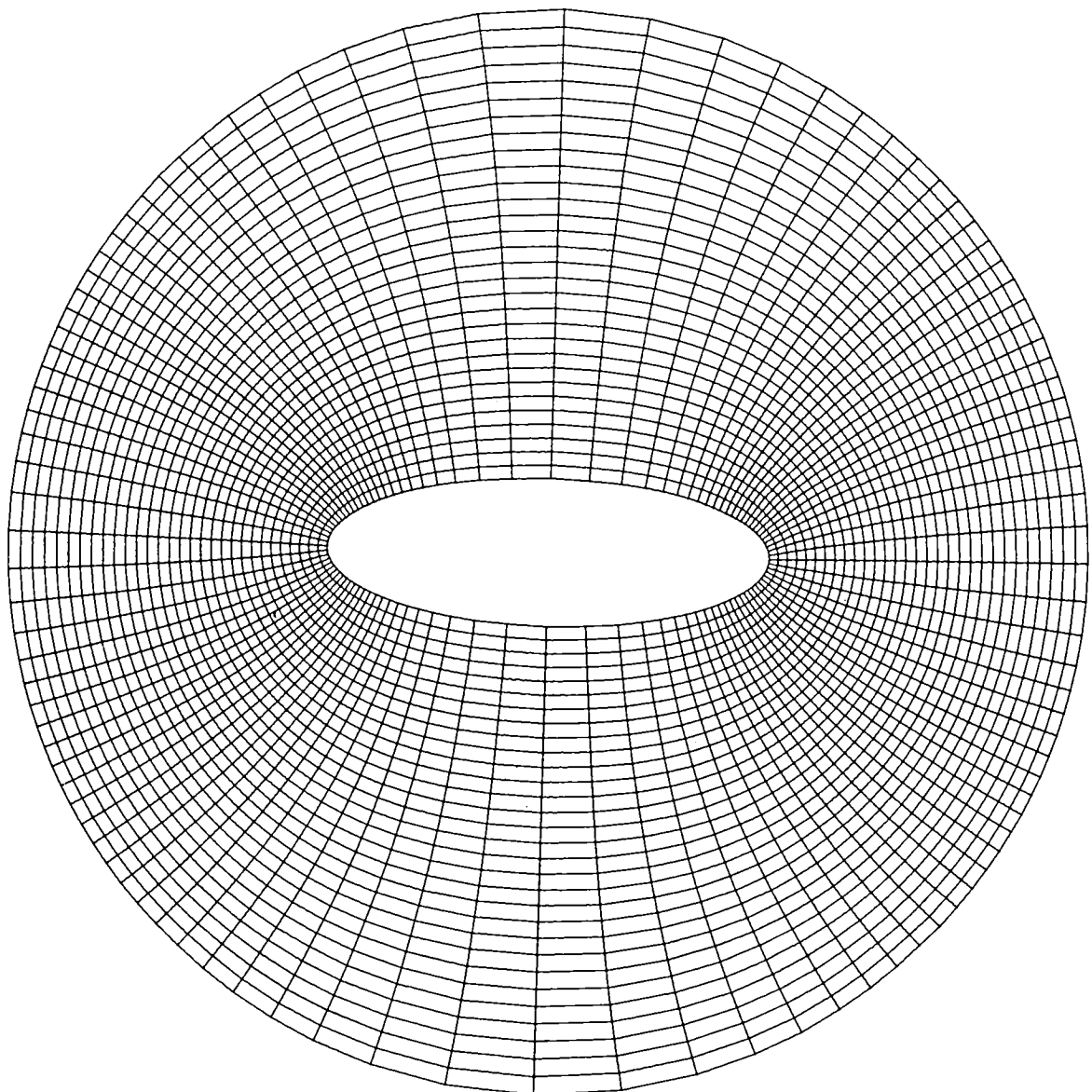


Figure 9.- Orthogonal coordinate system about 3:1 ellipsoid with unequal  $\xi$  spacing.

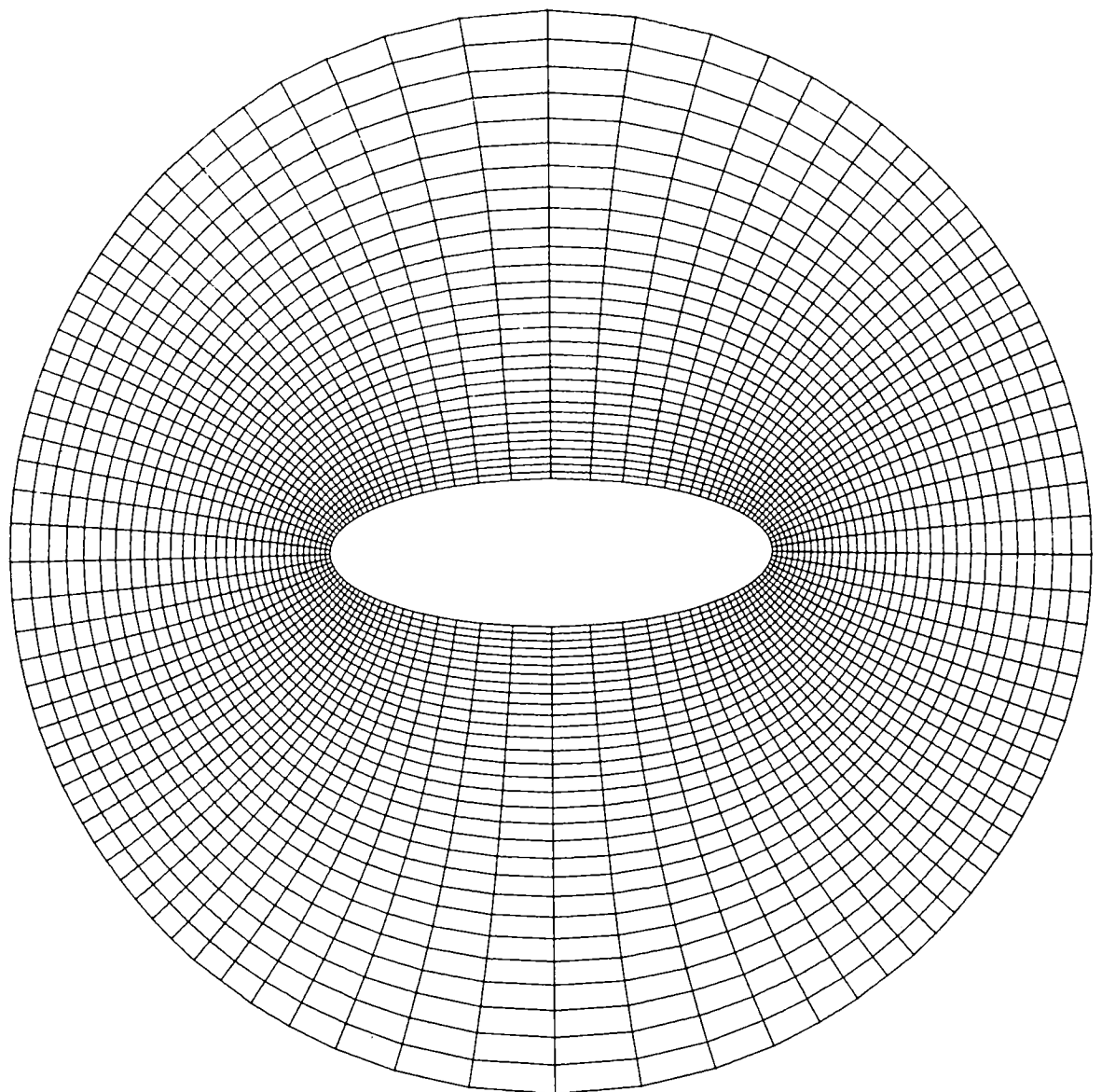


Figure 10.- Orthogonal coordinate system about 3:1 ellipsoid with unequal  $\xi$  and  $\eta$  spacing.

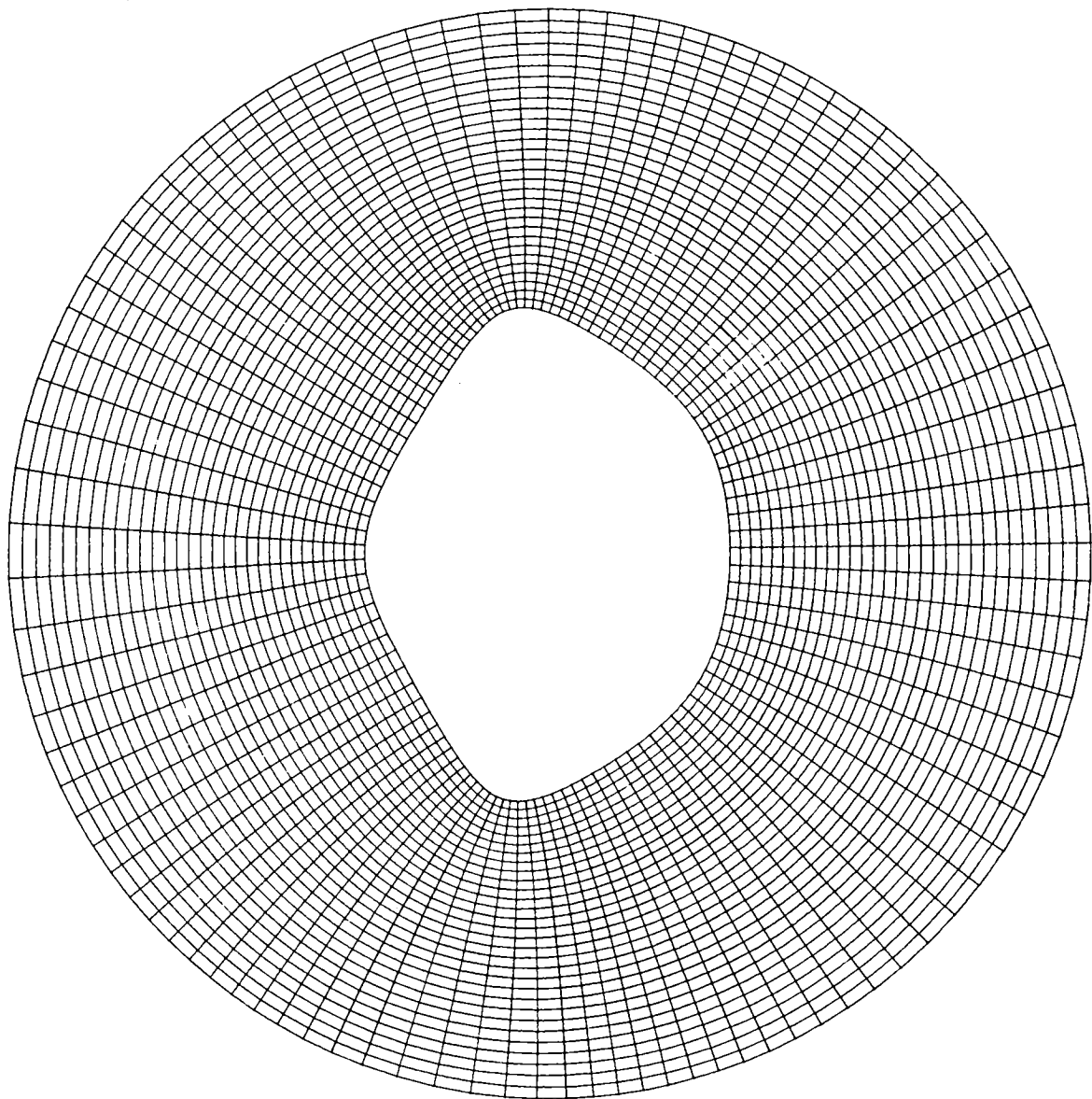


Figure 11.- Orthogonal coordinate system about planetary entry body.

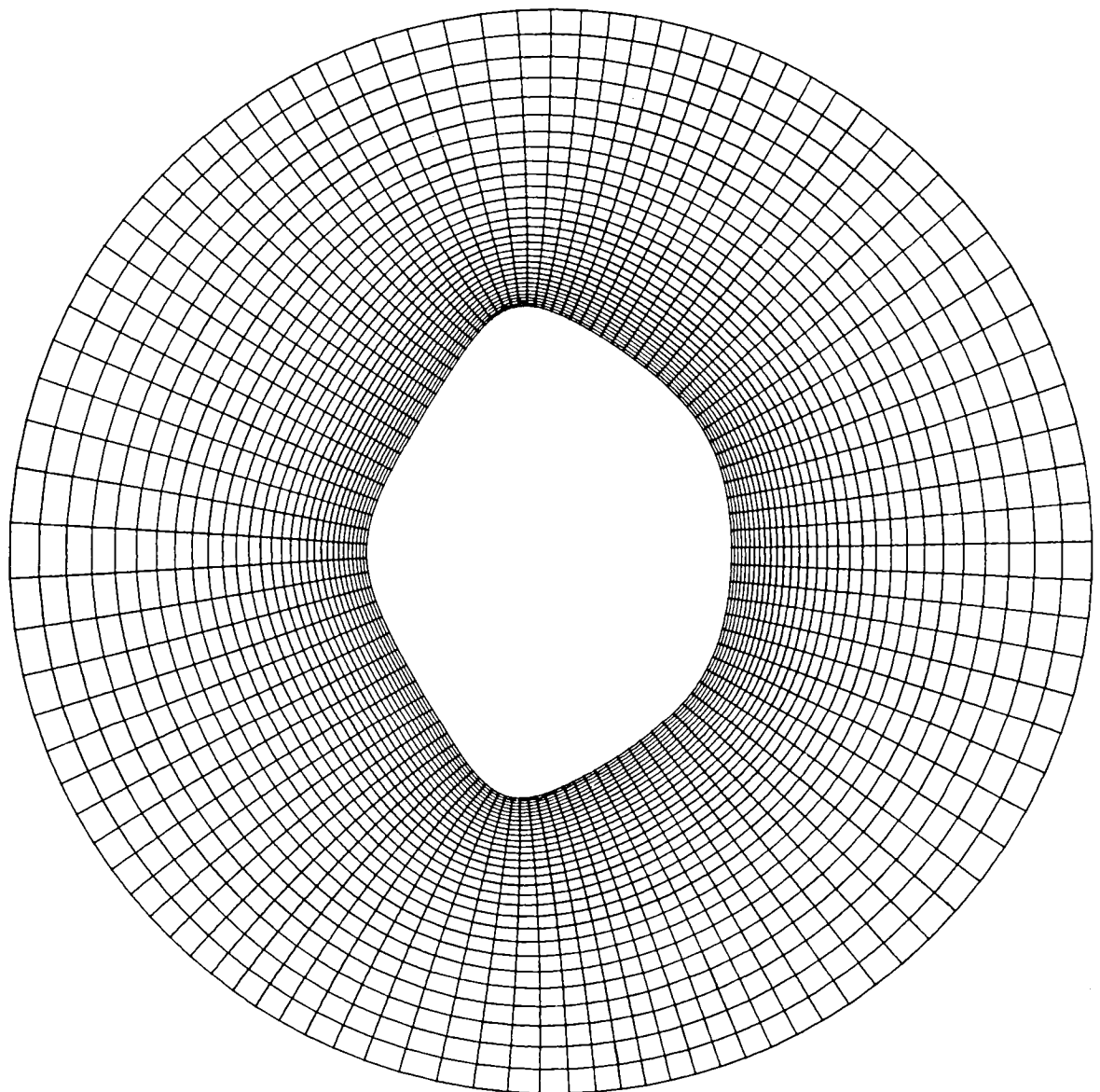


Figure 12.- Orthogonal coordinate system about planetary entry body with unequal  $\eta$  spacing.

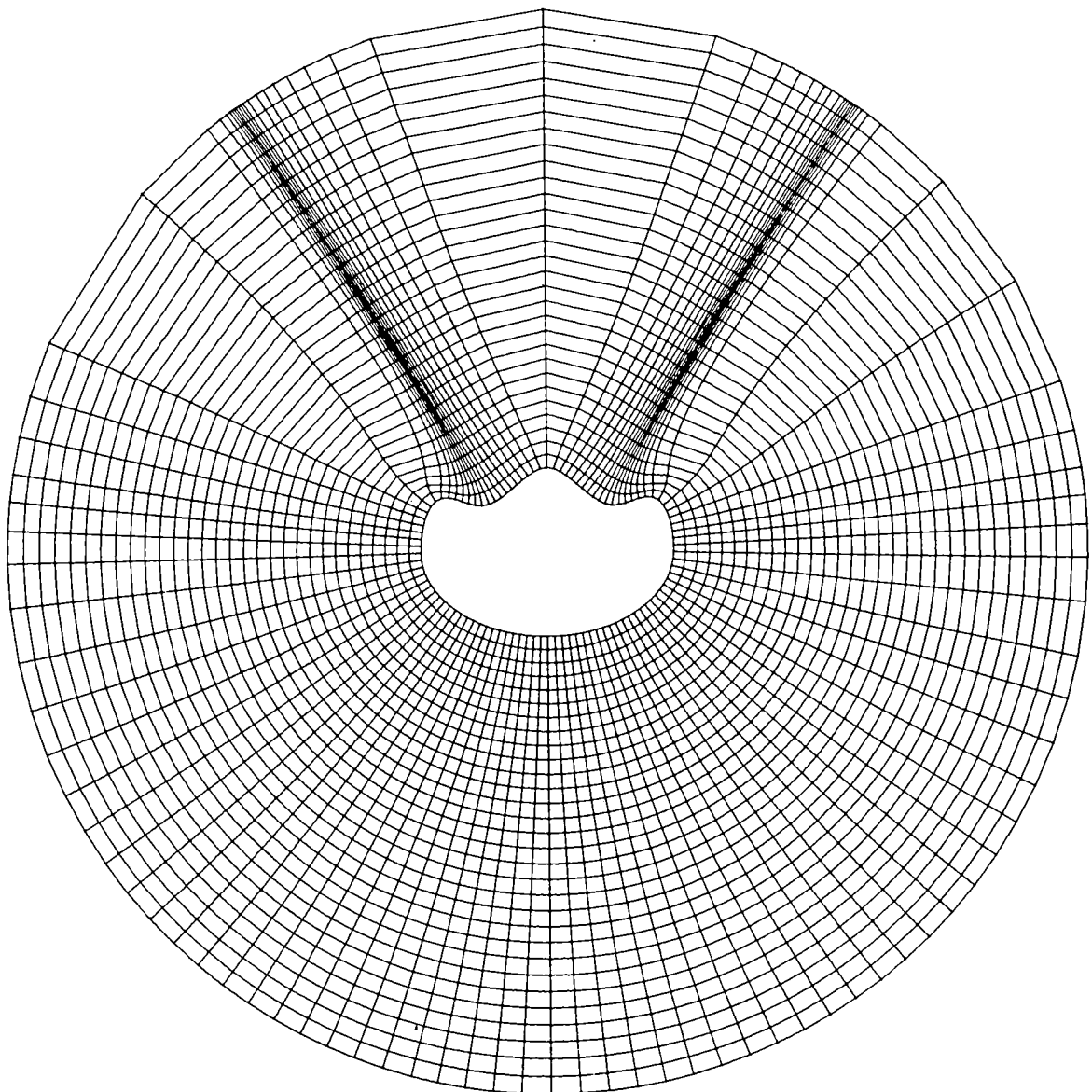


Figure 13.- Orthogonal coordinate system about arbitrary body with reverse curvature.

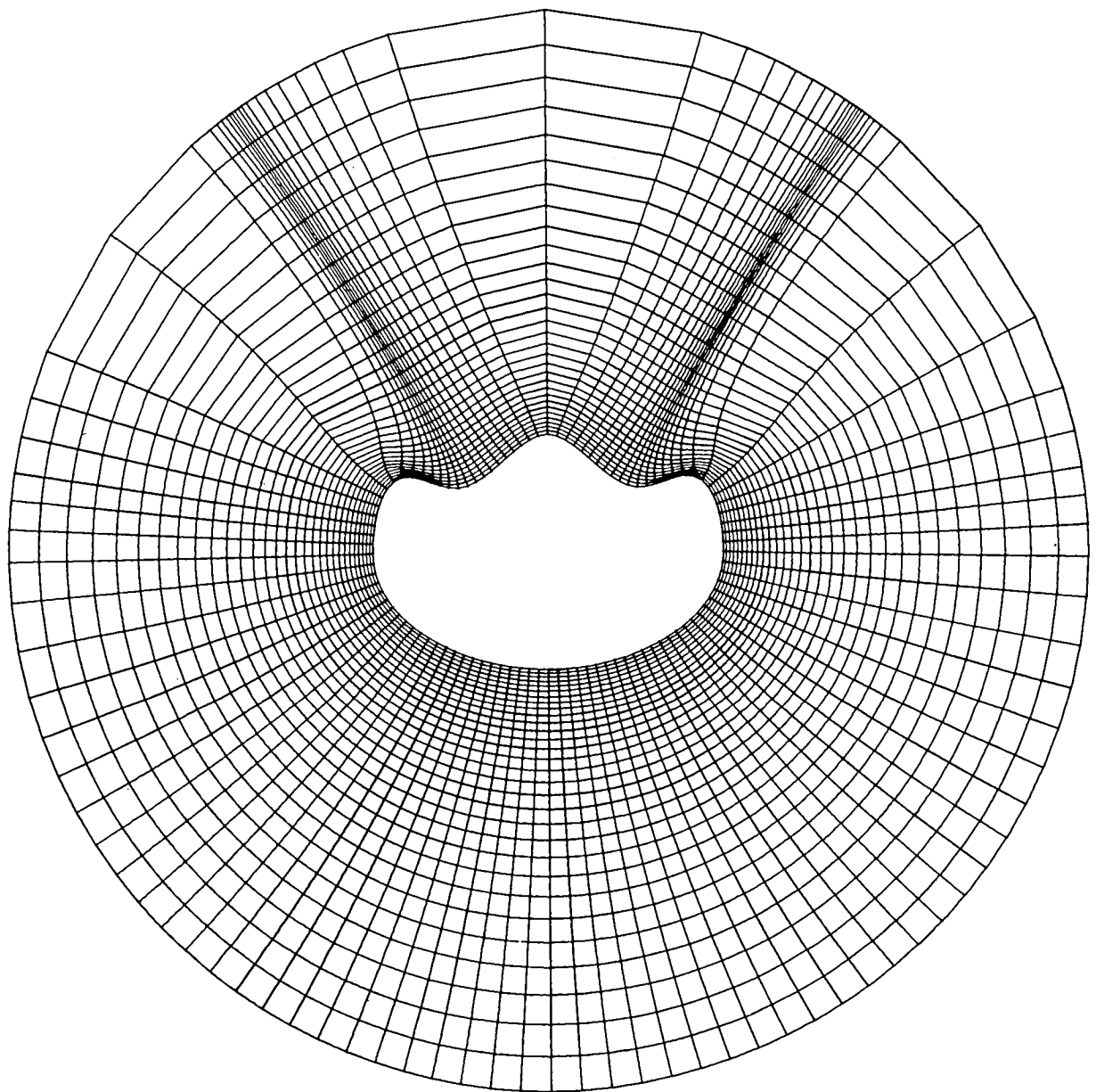


Figure 14.- Orthogonal coordinate system about arbitrary body with reverse curvature and unequal spacing in  $\eta$  direction.

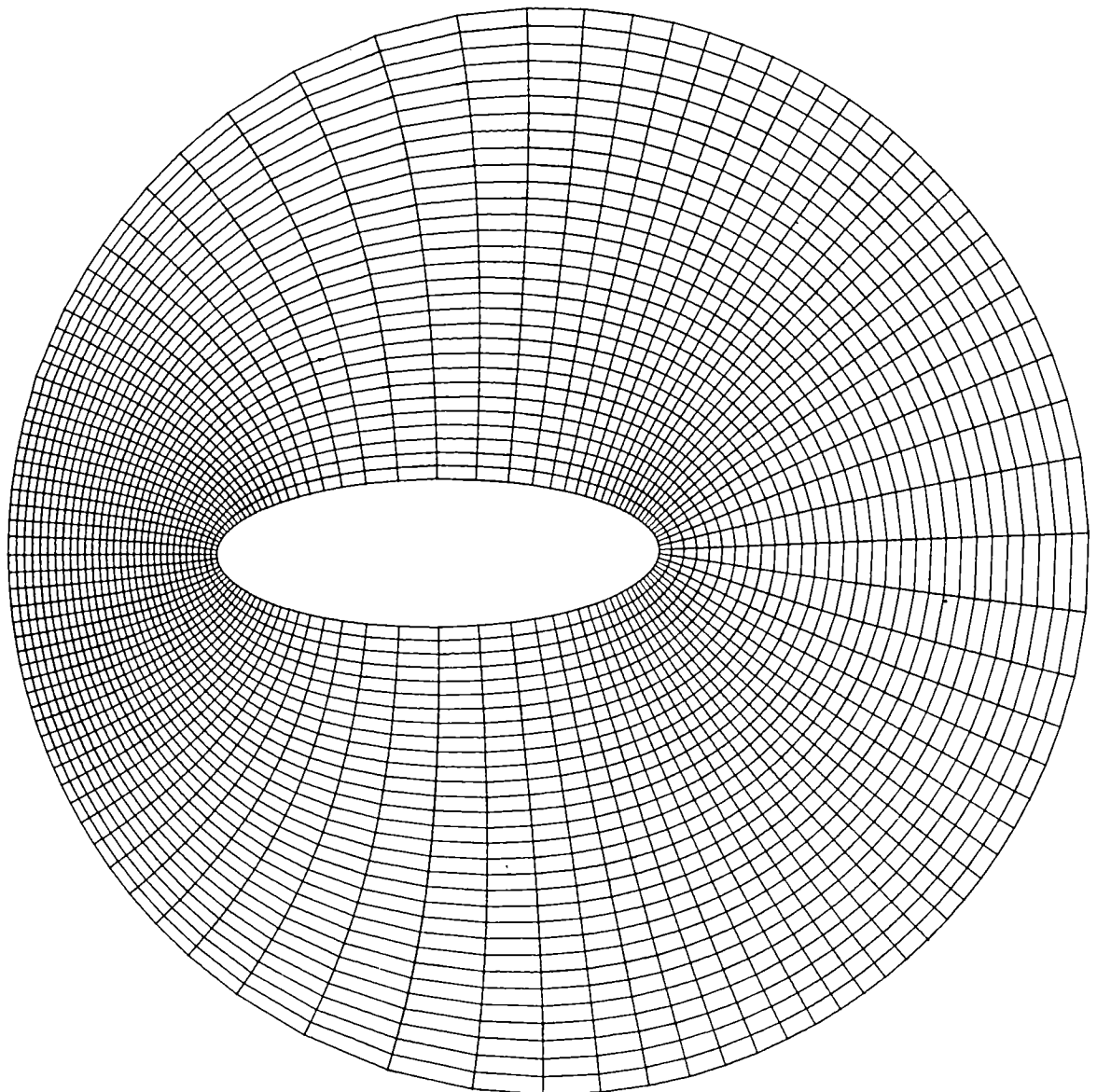


Figure 15.- Orthogonal coordinate system about 3:1 ellipsoid with displaced outer boundary and unequal  $\xi$  spacing.

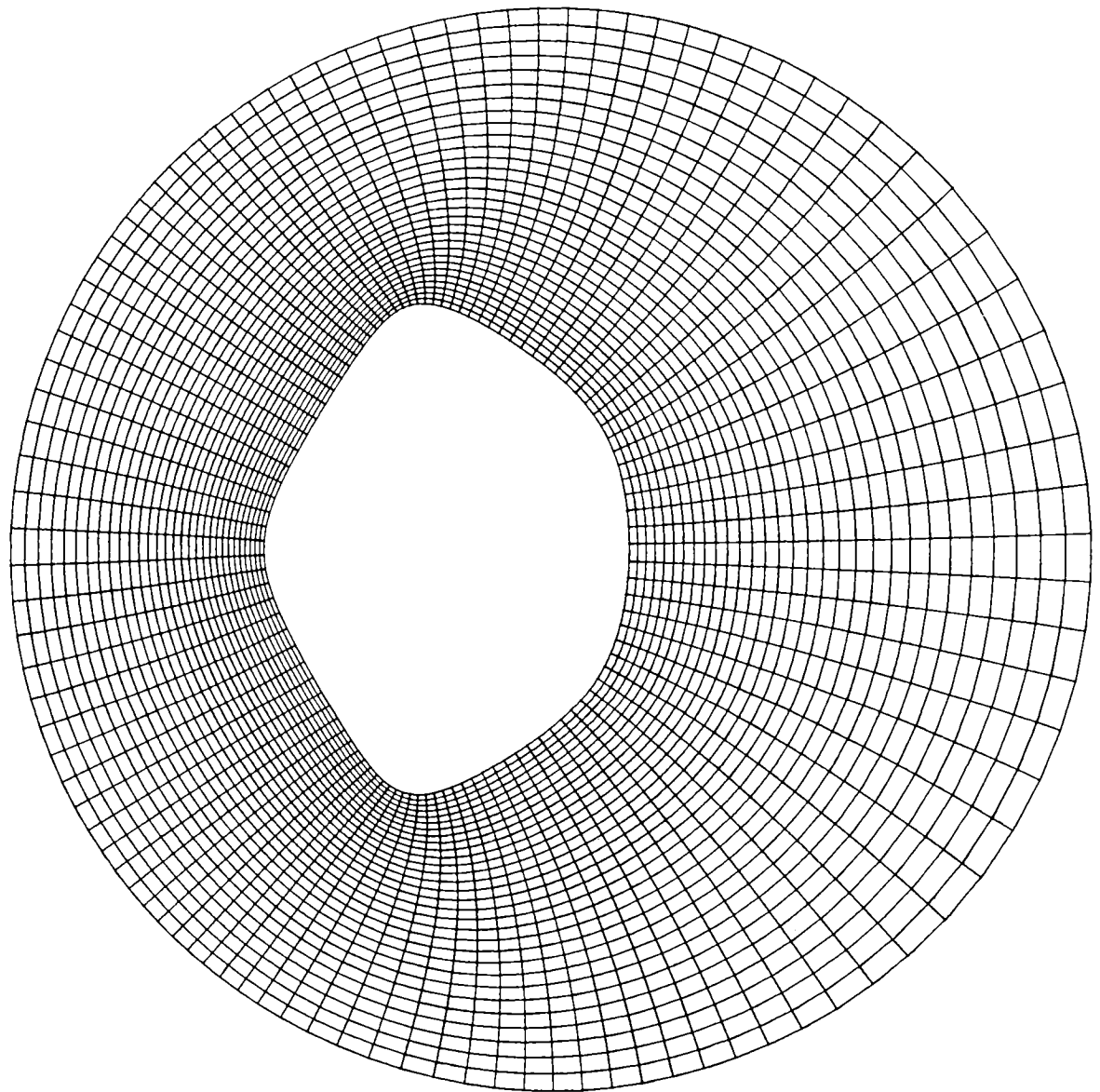


Figure 16.- Orthogonal coordinate system about planetary entry body with displaced outer boundary and unequal  $\eta$  spacing.

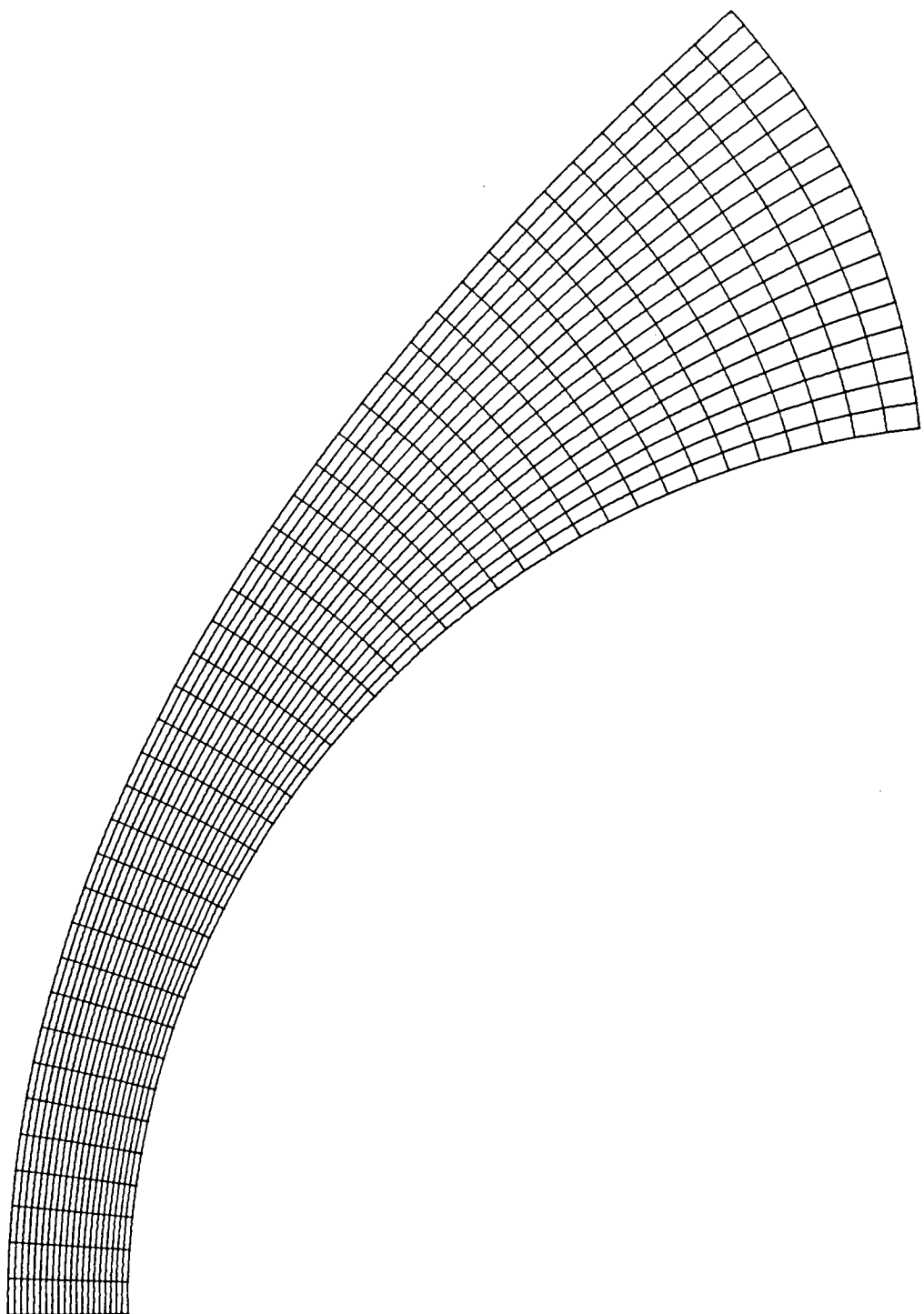


Figure 17.- Orthogonal coordinate system on forebody of spheroid.

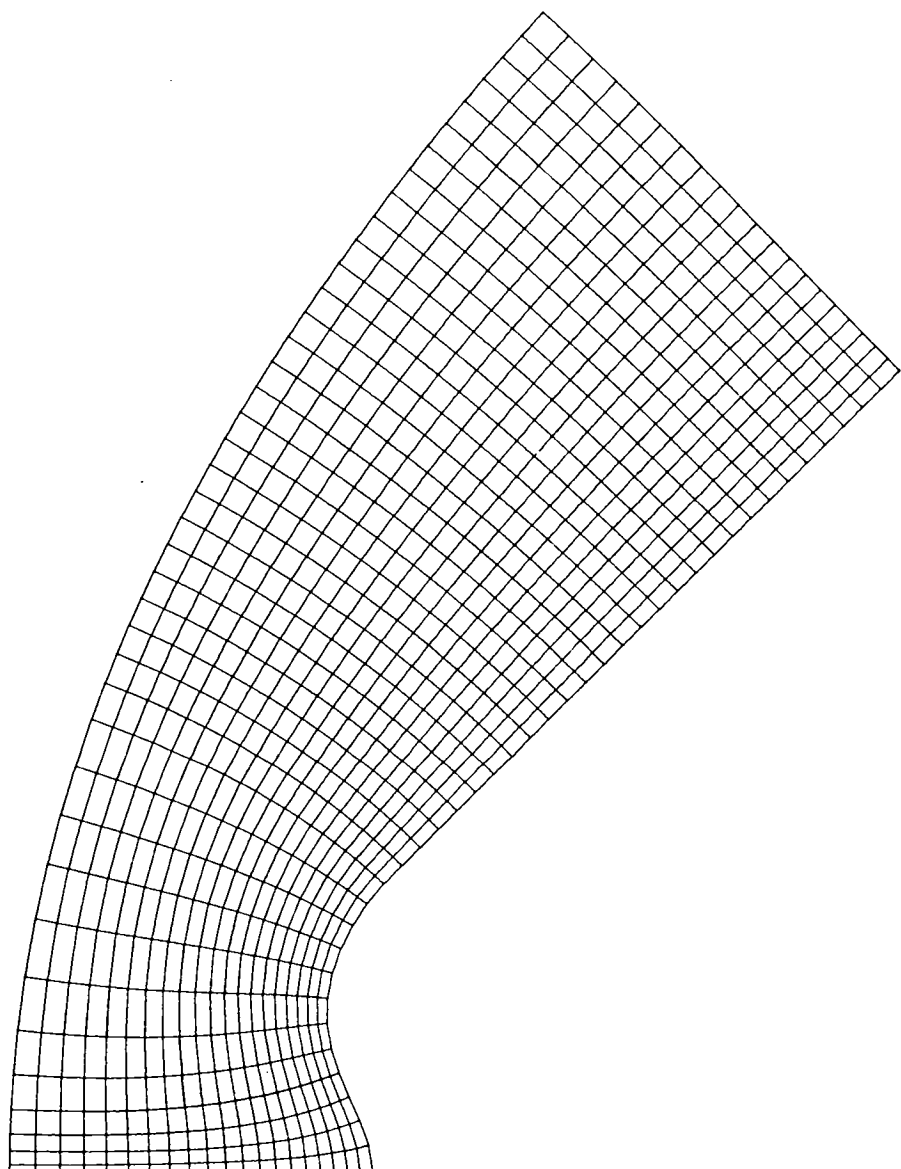


Figure 18.- Orthogonal coordinate system on forebody of reverse curvature conical body with unequal  $\eta$  spacing.

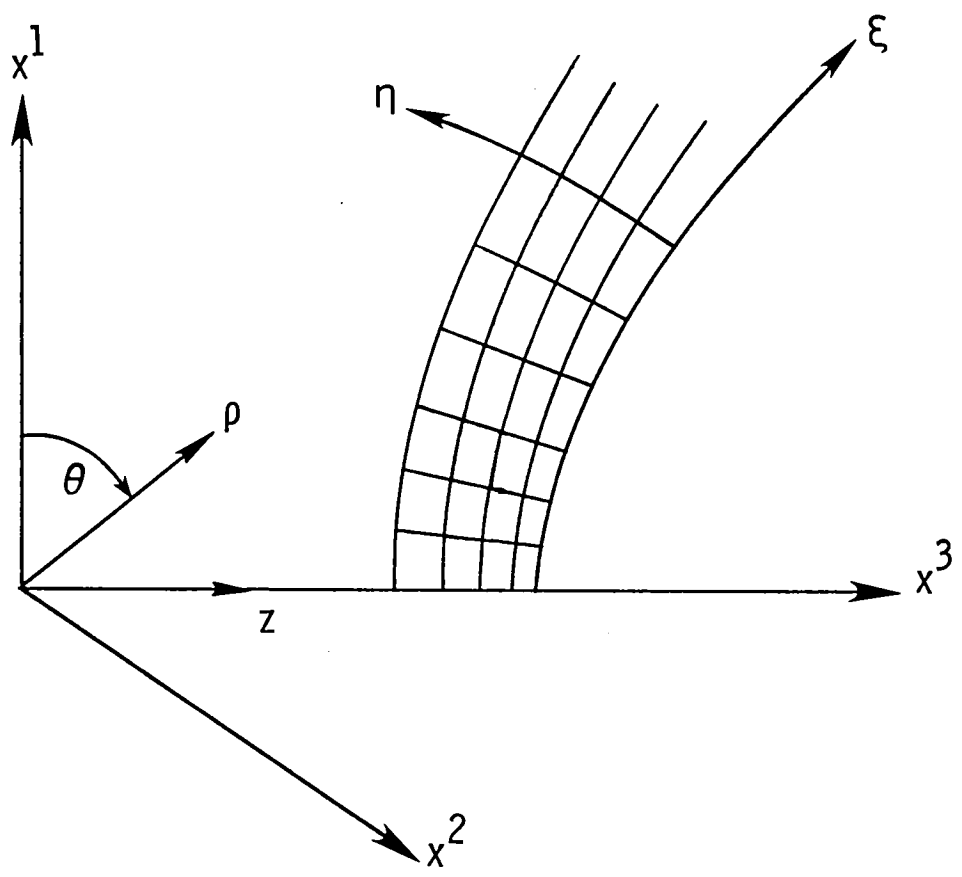


Figure 19.- Coordinate systems schematic.





1. Report No. NASA TM-80131	2. Government Accession No.	3. Recipient's Catalog No.	
4. Title and Subtitle <b>APPLICATION OF A NUMERICAL ORTHOGONAL COORDINATE GENERATOR TO AXISYMMETRIC BLUNT BODIES</b>		5. Report Date <b>October 1979</b>	6. Performing Organization Code
7. Author(s) <b>Randolph A. Graves, Jr.</b>		8. Performing Organization Report No. <b>L-13109</b>	10. Work Unit No. <b>506-26-13-01</b>
9. Performing Organization Name and Address <b>NASA Langley Research Center Hampton, VA 23665</b>		11. Contract or Grant No.	13. Type of Report and Period Covered <b>Technical Memorandum</b>
12. Sponsoring Agency Name and Address <b>National Aeronautics and Space Administration Washington, DC 20546</b>		14. Sponsoring Agency Code	
15. Supplementary Notes			
16. Abstract  An application of a simple numerical technique which allows for the rapid construction of orthogonal coordinate systems about axisymmetric blunt bodies is presented. This technique can generate orthogonal meshes which have unequally spaced points in two directions. Relations are given for the numerical generation of the metric coefficients. Body shapes ranging from simple analytical bodies to complex reverse curvature bodies are presented together with their orthogonal coordinate systems. The relatively good accuracy of the technique is shown in tabular data describing coordinate line slopes and metric coefficients. The "predictor-corrector" numerical method used to generate these results is both simple in concept and easy to program, so that the application of the technique should be broader than the results presented.			
17. Key Words (Suggested by Author(s))  Coordinates Orthogonal Numerical analysis Axisymmetric bodies		18. Distribution Statement  Unclassified - Unlimited  <b>Subject Category 64</b>	
19. Security Classif. (of this report)  Unclassified	20. Security Classif. (of this page)  Unclassified	21. No. of Pages  39	22. Price*  \$4.50

\* For sale by the National Technical Information Service, Springfield, Virginia 22161

NASA-Langley, 1979



National Aeronautics and  
Space Administration

Washington, D.C.  
20546

Official Business  
Penalty for Private Use, \$300

SPECIAL FOURTH CLASS MAIL  
BOOK

Postage and Fees Paid  
National Aeronautics and  
Space Administration  
NASA-451



NASA

POSTMASTER: If Undeliverable (Section 158  
Postal Manual) Do Not Return

---